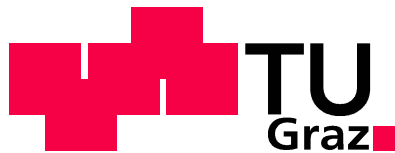


**Manufacturing Antibody Fragments -**  
Establishment of a Method Toolbox for Chromatographic  
Downstream Steps

**Diploma Thesis**

by  
Elisabeth Salomon



Graz University of Technology  
Biotechnology, Bio- and Food Chemistry

Accomplished at Boehringer Ingelheim RCV GmbH & Co KG

Supervised by Univ.-Prof. Dipl.-Ing. Dr.techn. Helmut Schwab  
Institute of Molecular Biotechnology, Graz University of Technology

Mai 2010

## STATUTORY DECLARATION

I declare that I have authored this thesis independently, that I have not used other than the declared sources / resources, and that I have explicitly marked all material which has been quoted either literally or by content from the used sources.

.....

date

.....

(signature)

# Acknowledgements

Special thanks to

Boehringer Ingelheim RCV GmbH & Co KG enabling this diploma thesis,

Dr. Matthias Berkemeyer and Dr. Helmut Schwab for their scientific support,

Dr. Marlene Zandian and DI Elena Vasilieva for mentoring and answering every little question that came up during work,

the whole unit of Downstream Process Science for the great working atmosphere and their encouragement,

my parents and my grandmother for believing in me.

Hans, thank you for being by my side.

# Table of Contents

Acknowledgements .....	- 3 -
Table of Contents .....	- 4 -
1 Abstract.....	- 7 -
2 Zusammenfassung .....	- 8 -
3 Introduction .....	- 10 -
3.1 Antibodies.....	- 10 -
3.1.1 Antibody Fragments .....	- 11 -
3.1.2 V <sub>HH</sub> Domain Antibodies .....	- 12 -
3.1.3 Yeast expression system: Pichia pastoris .....	- 15 -
3.2 Downstream Process .....	- 16 -
3.2.1 Chromatography in General .....	- 16 -
3.2.2 Mixed Mode Chromatography .....	- 17 -
3.3 Design of Experiments - DoE.....	- 19 -
4 Materials and Methods .....	- 21 -
4.1 Media .....	- 21 -
4.1.1 Chemicals .....	- 21 -
4.1.2 Water .....	- 21 -
4.1.3 Vectors and Organisms.....	- 21 -
4.1.4 Model Protein .....	- 21 -
4.2 Analytical Methods .....	- 22 -
4.2.1 UV-VIS Spectroscopy .....	- 22 -
4.2.2 LDS-PAGE.....	- 22 -
4.2.3 Coomassie Simply Blue Safe Staining .....	- 23 -
4.2.4 Silver Staining .....	- 23 -
4.2.5 Protein A - HPLC .....	- 24 -
4.2.6 IEX - HPLC .....	- 24 -
4.2.7 SEC - HPLC .....	- 24 -
4.2.8 RP - HPLC.....	- 25 -
4.3 Fermentation.....	- 25 -
4.3.1 Dry Cell Weight (DCW).....	- 26 -
4.3.2 Optical Density (OD <sub>550</sub> ) .....	- 26 -

4.4	Primary recovery .....	- 26 -
4.5	Adsorption Isotherms .....	- 27 -
4.6	Chromatography .....	- 28 -
4.6.1	Äkta Chromatography Station .....	- 28 -
4.6.2	Column Packing .....	- 29 -
4.6.3	Column Evaluation .....	- 30 -
5	Objectives .....	- 31 -
6	Results and Discussion .....	- 32 -
6.1	Clone Screening .....	- 32 -
6.2	Fermentation .....	- 32 -
6.3	Downstream Process Development .....	- 34 -
6.3.1	Capture Step .....	- 34 -
6.3.1.1	MabSelect Xtra .....	- 34 -
6.3.1.2	Blue Sepharose 6FF .....	- 36 -
6.3.2	Evaluation of Affinity Media .....	- 40 -
6.3.2.1	Breakthrough Curves .....	- 40 -
6.3.2.2	Binding Capacities .....	- 42 -
6.3.2.3	Adsorption Isotherms .....	- 45 -
6.3.3	Intermediate Step .....	- 47 -
6.3.3.1	HIC - Phenyl Sepharose HP .....	- 47 -
6.3.3.2	HIC – Toyopearl Phenyl 600-M .....	- 49 -
6.3.3.3	AIEX - Fractogel EMD TMAE .....	- 50 -
6.3.3.4	AIEX - Q Sepharose FF .....	- 51 -
6.3.3.5	AIEX - DEAE Sepharose FF .....	- 52 -
6.3.3.6	CIEX - Fractogel EMD SO <sub>3</sub> .....	- 52 -
6.3.3.7	CIEX - SP Sepharose HP .....	- 54 -
6.3.3.8	CIEX - CM Sepharose HP .....	- 56 -
6.3.4	Present Downstream Process .....	- 60 -
6.4	Downstream Process - Alternatives .....	- 62 -
6.4.1	Intermediate Step – Mixed Mode Resins .....	- 62 -
6.4.1.1	Capto MMC .....	- 62 -
6.4.1.2	HEA HyperCel .....	- 68 -
6.4.1.3	PPA HyperCel .....	- 69 -
6.4.1.4	MEP HyperCel .....	- 70 -

6.4.2	Mixed Mode vs. CM Sepharose HP .....	- 71 -
7	Conclusions and Perspectives.....	- 74 -
8	Abbreviations .....	- 75 -
9	Reference .....	- 77 -
10	Index of Figures.....	- 83 -
11	Index of Tables .....	- 86 -

## ***1 Abstract***

As a promising alternative to conventional antibodies, antibody fragments have been engineered in the recent years. Because of their small size, the production in different microbial host formats is enabled, thus leading to different requirements in purification processes, focusing on high purities while maintaining low costs. The present work was focused on the purification of the domain antibody  $V_{HH3}$ , which is derived from the camelidae family.  $V_{HH3}$  dimer is fused to HSA at the C-terminus, which is required to extend the half-life of the protein. First, a downstream purification process had to be developed. Different chromatography media were screened, with the final selection of the HSA-affinity resin Blue Sepharose 6FF as capture step and CM Sepharose HP as intermediate step resin. Determined binding capacities and kinetic parameters of the tested affinity resins confirmed the decision of Blue Sepharose 6FF as capture step. In order to test practicality, the entire downstream process, including formulation was performed with an overall yield of 39.0 %. Purity varied between 78.1 to 98 %, depending on the analytical methods applied. Implementation of CM Sepharose HP made a desalting step necessary between the purification steps, leading to an extend in time and costs. Hence screening for an alternative intermediate step resin was performed. Because various conventional resins, including HIC, CIEX and AIEX media, were already screened in process development, a novel option of chromatographic media - mixed-mode resins - was investigated. These mixed-mode resins are designed with multi-modal operating ligands allowing the possibility that adsorption takes place at high salt concentrations, making them an ideal replacement of CM Sepharose HP. Four different mixed-mode resins were tested (Capto MMC, PPA HyperCel, HEA HyperCel and MEP HyperCel), applying Design of Experiments (DoE), a statistical method, in the development of Capto MMC. Mixed-mode media were comparable to CM Sepharose HP with regard to yield and purity as analyzed by LDS-PAGE (Coomassie and silver stained) and RP-HPLC. Only purity analyzed by CIEX-HPLC is lower (64.7 to 79.4 % compared to 96.0 %), indicating protein isoforms which are separated on CM Sepharose HP, hence optimization of mixed-mode resins is still necessary. The yields obtained varied between 76.3 to 104.7 % compared to 84.0 % for CM Sepharose HP indicating that these novel media are a real alternative to the present purification process of  $V_{HH3}$ .

## 2 Zusammenfassung

Als vielversprechende Alternative zu herkömmlichen Antikörpern haben sich in den letzten Jahren Antikörperfragmente etabliert. Wegen ihrer geringen Größe ist die Produktion in verschiedensten mikrobiellen Wirtssystemen möglich. Es kommt dadurch zu unterschiedlichen Anforderungen an den Reinigungsprozess mit Fokus auf hohe Reinheiten und geringe Kosten. Diese Arbeit konzentrierte sich auf die Reinigung des Domän-Antikörpers  $V_{HH3}$ , der aus der Familie der Camilidae isoliert wurde.  $V_{HH3}$  ist ein Dimer mit HSA am C-Terminus, welches die Halbwertszeit des Proteins *in vivo* verlängert. Als erstes wurde ein Downstream Reinigungsprozess entwickelt. Dafür wurden verschiedene Chromatographiemedien getestet. Ausgewählt wurde das HSA-Affinitätsmedium Blue Sepharose 6FF für den Capture Schritt und CM Sepharose HP für den Intermediate Schritt. Die ermittelten Bindungskapazitäten und kinetischen Parameter der getesteten Affinitätsmedien bestätigten die Wahl von Blue Sepharose 6FF als Capture Schritt. Der Gesamtprozess inklusive Formulierung wurde daraufhin durchgeführt um dessen Anwendbarkeit auszutesten. Es ergab sich eine Gesamtausbeute von 39 % mit Reinheiten die zwischen 78.1 und 98 % in Abhängigkeit der Analysenmethode schwankten. Die Verwendung von CM Sepharose HP machte einen Entsalzungsschritt zwischen den Reinigungsschritten notwendig, was zu einer längeren Prozessdauer und zu höheren Kosten führt. Es wurde daher nach einem Alternativen Medium für den Intermediate Schritt gesucht. Weil verschiedenste konventionelle Medien wie HIC, CIEX und AIEX schon in der Prozessentwicklung getestet wurden, wurden neuartige Mixed-Mode Medien untersucht. Diese Gele besitzen multi-modale Liganden mit der Möglichkeit der Adsorption auch bei hohen Salzkonzentrationen und stellen daher ein idealen Ersatz für CM Sepharose HP dar. Vier verschiedene Mixed-Mode Medien wurden getestet (Capto MMC, PPA HyperCel, HEA HyperCel und MEP HyperCel) und für die Entwicklung der Capto MMC Methode wurde Design of Experiments (DoE), eine statistische Methode angewendet. Mixed-Mode Gele ergaben ähnliche Ergebnisse wie CM Sepharose HP bei der Analyse von Ausbeute und Reinheit mittels LDS-PAGE (Coomassie- und Silberfärbung) und RP-HPLC. Nur die Reinheit analysiert mit CIEX-HPLC war geringer (64.7-79.4 % zu 96.0 %), was auf Isoformen hinweist die mittels CM Sepharose HP abgetrennt wurden. Dies macht eine weitere Optimierung der Mixed-Mode Medien notwendig. Die mit LDS-PAGE berechneten



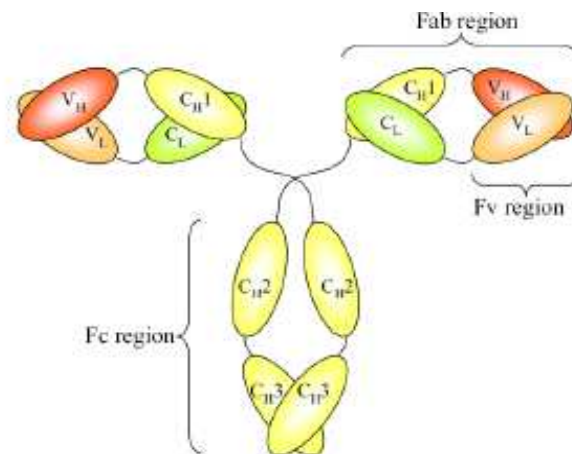
Ausbeuten schwankten zwischen 76.3 und 104.7 % zu 84.0 % bei CM Sepharose HP. Die erhaltenen Ergebnisse machen diese neuartigen Chromatographiemedien zu einer sehr guten Alternative im derzeitigen Reinigungsprozess von  $V_{HH3}$ .

## 3 Introduction

### 3.1 Antibodies

Antibodies, belonging to the family of immunoglobulin (Ig), are glycoproteins that play a key role in the immune response of all living organisms. In the humoral immune response they bind to recognition elements, called epitopes, of pathogens (antigens), such as bacteria, viruses, larger parasites with high specificity. These marked invaders are then killed by the cellular immune response comprising of T cells [J. M. Berg et al., 2002].

There are five different immunoglobulin classes: IgA, IgD, IgE, IgG and IgM. For describing the antibodies structure immunoglobulin G (IgG) is most commonly referred to, as it is the immunoglobulin that is present in highest concentration in the serum and mostly used as a therapeutic agent [Joosten et al., 2003]. The IgG molecule is composed out of four chains: two heavy (H-) chains, with each 50 kDa and two light (L-) chains with each 25 kDa (Figure 1).



**Figure 1: Composition of an IgG antibody [Joosten et al.]**

The whole subunit composition is L<sub>2</sub>H<sub>2</sub> and the chains are linked together with disulfide bridges and non-covalent bonds. The light chain is composed of one variable (V<sub>L</sub>) and one constant domain (C<sub>L</sub>), whereas the heavy chain is made of one variable domain (V<sub>H</sub>) and three constant domains (C<sub>H</sub>1, C<sub>H</sub>2, and C<sub>H</sub>3) [Alberts et al., 2002].

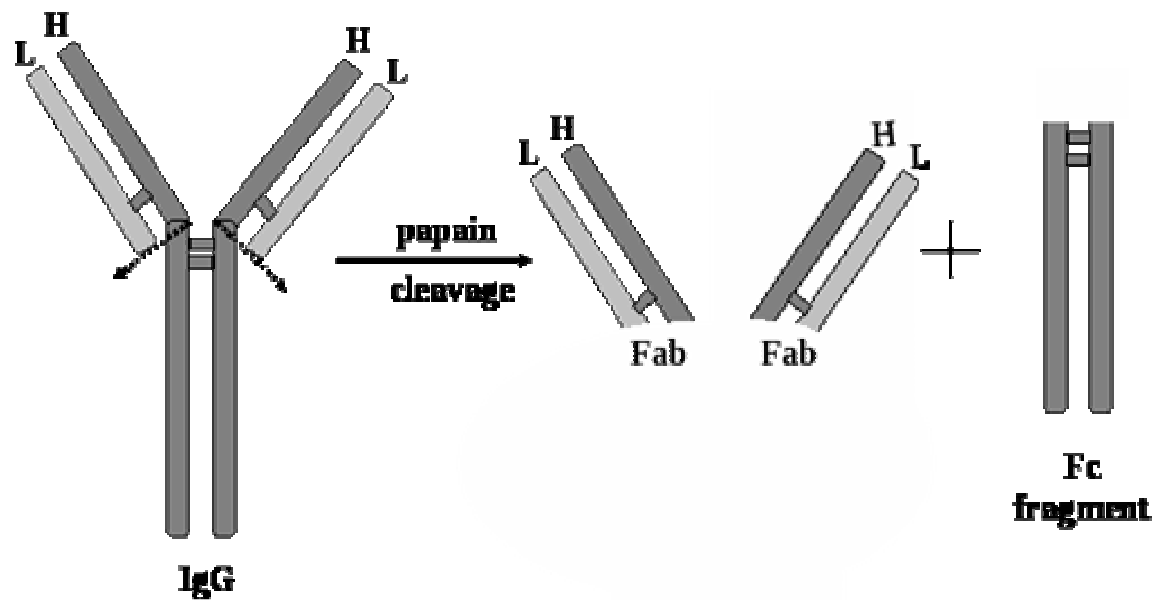


Figure 2: Structure of an IgG antibody with its three active fragments [http://www.secondary-antibody.com]

IgG can be cleaved by proteolytic activity of papain into three 50 kDa fragments that still remain active. In Figure 2 this cleavage is shown. Heavy and light chains are connected in two so called  $F_{ab}$ -fragments (**F**ragment **a**ntigen **b**inding) that bind antigen. They are also called “variable regions”, because they are different from antibody to antibody. These Fab-domains are linked to the  $F_c$ -region (**F**ragment **c**rystallizing or **c**onstant) that has no binding activity but mediates the initiation of a cascade that leads to the lysis of target cells [J. M. Berg et al., 2002].

### 3.1.1 Antibody Fragments

In general there are two trends in development of novel antibody formats: reduction of size and the improvement of antibody properties. An example for size reduction is the camelid heavy-chain antibody ( $V_{HH}$ ) which has a molecular weight of 15 kDa [Joosten et al., 2003]. The nomenclature of antibodies and its fragments is based on the domains that are included (Figure 3).

For pharmaceutical and biotechnological applications, reactions initiated by the  $F_c$ -region are not always important. Consequently, antibody fragments that lack this region were constructed: monovalent single chain fragments ( $scF_c$ ) antigen-binding fragments ( $F_{ab}$ ) and also engineered antibody fragments, such as diabodies, triabodies, minibodies, and single-domain antibodies [Holliger and Hudson, 2005]. Genetic improvements resulted in a high diversity of antibody fragments with new characteristics such as enhanced specificity, therapeutic efficiency, and stability [Schmitz et al., 2000].

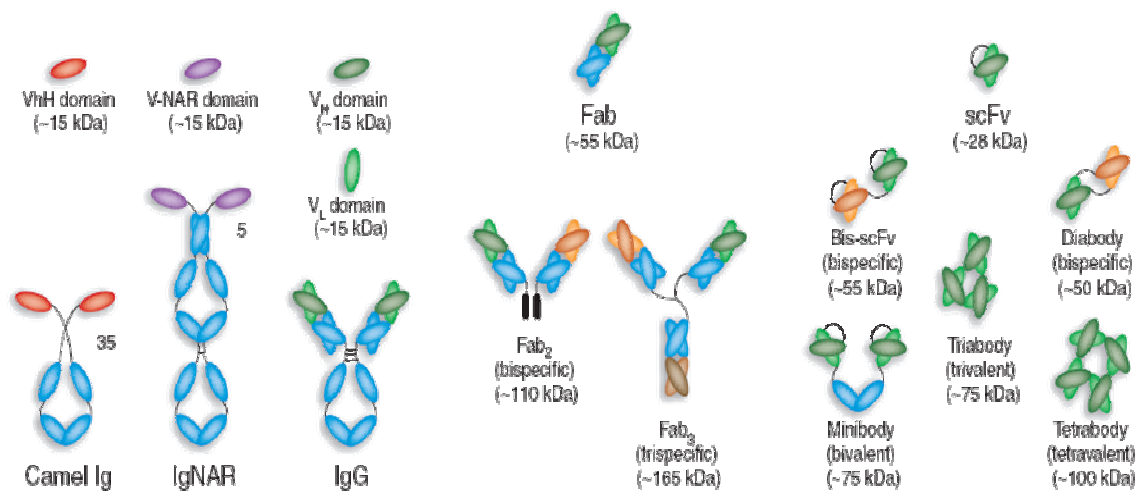
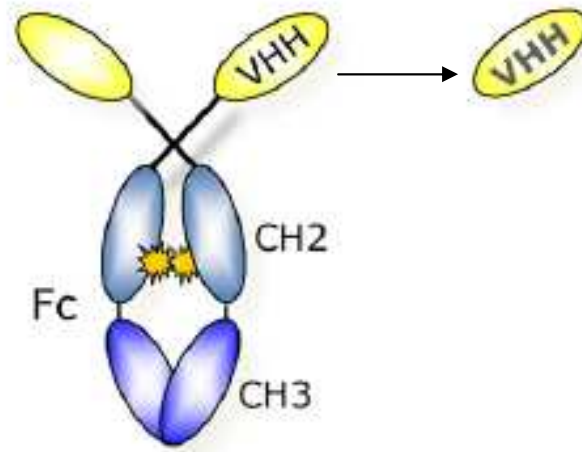


Figure 3: Variation of antibody fragments [P. Holliger et al., 2005]

### 3.1.2 $V_{HH}$ Domain Antibodies

Camelidae, consisting of camels, dromedaries, alpacas and llamas, feature unique antibodies only consisting of heavy chains with a single N-terminal domain ( $V_{HH}$ ) shown in Figure 4. Camelid heavy-chain antibodies have the complete functionality and the  $V_{HH}$ -domain alone is able to bind antigen solely [Hamers-Casterman et al., 1993]. These heavy-chain antibodies are missing both light chains and the  $C_{H1}$  domain because of a splice site mutation [M. M. Harmsen and H. J. DeHaard, 2007]. The remaining  $C_H$  domains ( $C_{H2}$  and  $C_{H3}$ ) form an  $F_c$ -equivalent constant domain framework [Holliger and Hudson, 2005].

However, heavy-chain antibodies, as well as isolated  $V_{HH}$  domains, exhibit a strong antigen-binding capacity, suggesting that the antibody is able to compensate for the lack of  $V_L$  domains [S. Muyldermans, 2001].



**Figure 4: Camelid heavy chain antibody and  $V_{HH}$  domain antibody [S. Muyldermans et al., 2009]**

In fact,  $V_{HH}$  domains are encoded by a separate set of approximately 40 gene segments that are responsible for modifications that compensate the lack of  $V_L$  and that show significant differences compared with conventional  $V_H$  gene segments [V. K. Nguyen et al., 2000; S. Muyldermans, 2001].

$V_{HH}$  domain antibodies possess unique characteristics compared to conventional antibody fragments and therefore makes them highly interesting for the use in novel therapeutic opportunities [F. van Bocksteale et al., 2009].

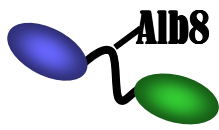
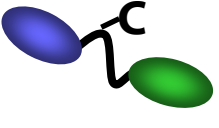
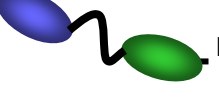
$V_{HH}$  antibody fragments are usually well expressed in microorganisms such as *E. coli* [M. Arbabi Ghahroudi et al., 1997] and *S. cerevisiae* [L. G. Frenken et al., 2000]. In the last years other hosts were also successfully used, including mammalian systems [M. R. Bazl et al., 2007] *P. pastoris* [K. Omidfar et al., 2007; F. Rahbarizadeh et al., 2006] and as well different plant species [A. Ismaili et al., 2007; S. A. Jobling et al., 2003].

$V_{HH}$  antibodies are able to penetrate cavities in target antigens like enzyme active sites and are also able to recognize cryptic epitopes that are not accessible to conventional antibodies [B. Stijlemans et al., 2004; Stanfield et al., 2004]. Their small size - 15 kDa - reduces the incidence of non-specific binding and moreover, camelid  $V_{HH}$  domain antibodies share a high sequence identity with their human  $V_H$  counterparts, thus leading to a decreased immunogenicity risk [K. B. Vu et al., 1997]. Because their size is below the renal filtration threshold of about 60 kDa, they are rapidly cleared from the blood with a serum half-life of approximately 1.5 h. With this short half-life  $V_{HH}$  domain antibodies are privileged for the development of therapeutic agents for acute indications in critical care medicine, including acute coronary syndrome (ACS) [V. Cortez-Retamozo et al., 2002].

On the other hand, they have to be adopted for medical applications that need a longer life time *in vivo*. Different half-life extending strategies are used, for example chemical addition of PEG (PEGylation) [M. M. Harmsen et al., 2007], the direct fusion to serum albumin [H. Revets et al., 2005] and also the linkage of domain antibodies, resulting in bi- or trispecific antibody fragments. In addition to enhancing the molecular weight these bi- or trispecific antibody fragments can be used to target multiple antigens.

Table 1 shows examples of half-life extension, with  $V_{HH}$  3 as the antibody fragment used in this work.

**Table 1: Examples for half-life extension**

$V_{HH}$ 1	Dimer with albumin binding site between the $V_{HH}$ domain antibodies	
$V_{HH}$ 2	Dimer with Cystein linker between the $V_{HH}$ domain antibodies	
$V_{HH}$ 3	Dimer with HSA at C-terminus	

$V_{HH}$ 's are highly stable, especially against heat [M. Arbabi Ghahroudi et al., 1997; R. H. van der Linden et al., 1999] and, even when molecules denature at melting points of 60 to 80°C, they have the unique ability to melt reversibly [S. Ewert et al., 2002; J. M. Perez et al., 2001],

compared to conventional antibody fragments, which aggregate irreversibly following denaturation. Also  $V_{HH}$  domain antibodies are resistant to other denaturing agents and conditions, such as detergents, guanidine hydrochloride, urea and high pressure [E. Dolk et al., 2005; M. Domoulin et al., 2002].

### **3.1.3 Yeast expression system: *Pichia pastoris***

In the last decade, the eukaryotic expression system *P. pastoris* has proven to be a prosperous host for the high-level production of a variety of heterologous proteins [Cregg et al., 2000]. More than 500 recombinant products have been produced in this host to this day. The many advantages that *P. pastoris* shows in protein expression are well reviewed [Macauley-Patrick et al., 2005] and include the ability to grow to high-cell-densities in minimal media and the presence of strong and strictly regulated promoters.

The most frequent used promoter for recombinant protein production is the methanol-inducible AOX1 promoter. As an alternative promoter glyceraldehyde phosphate dehydrogenase promoter (GAP) can also provide high expression levels and the potential of large-scale processes [Hohenblum et al., 2004], but the highest production yields are still reported for the AOX1 promoter [Cos et al., 2006].

*P. pastoris* can compete with heterologous protein expression in mammalian cells, because of its capability of performing post-translational modifications such as proteolytic processing, protein folding, formation of disulfide bonds and glycosylations, including N- and O-linked glycosylations. Although glycosylations in *P. pastoris* differ from the mammalian-type pattern (the glycosylation structures are limited to the high-mannose type), they are usually less hindering to protein folding than the hyperglycosylations of *S. cerevisiae* [Tschopp et al., 1987].

To overcome the glycosylation-disadvantage for production of pharmaceutical products, a lot of research is done in this field of study and recent improvements in the glycosylation-engineering have generated strains that can express homogeneously glycosylated, humanized proteins [Hamilton et al., 2003].

## **3.2 Downstream Process**

The design of a purification process depends on how the product is produced. Depending on the source of the product there are more or less by-products that have to be removed. Intracellular products first have to be released from the cells; mostly this is done with a high pressure homogenizer. The next step comprises extraction and refolding, or only extraction, depending if the product already has its native conformation. Secreted products will be centrifuged or filtrated, mainly both, as a first step. In either cases, secreted or not the product will undergo further purification steps that are most commonly based on chromatographic steps [R. Hahn, 2008].

### ***3.2.1 Chromatography in General***

For performing purification of proteins to a level of pharmaceutical grade several chromatographic steps with different principles of chemical interaction have to be carried out.

Traditionally “classic” chemical engineering methods like precipitation, extraction, crystallization, centrifugation etc. were used for purification of biomolecules. The adoption of preparative chromatography improved bioseparations, especially in respect to volume throughput and purity of products [J. C. Janson and L. Ryden, 1998; R. K. Scopes, 1994 ].

The basic principle of chromatography is due to the separation of solute molecules between two phases, most common for biotechnology a solid and a liquid phase [P. A. Bird et al., 2002]. Principle methods of bioseparation are hydrophobic interaction chromatography (HIC), reversed phase chromatography (RPC) [J. Porath et al., 1973], both with hydrophobic interaction as basic principle, affinity chromatography which takes advantage of the specific interaction of a biomolecule with its biologic counterpart [P. Cuatrecasas et al., 1967] and ion-exchange chromatography (IEX) that separates molecules by ionic binding depending on their surface charge. For size exclusion chromatography (SEC) separation is based on the exclusion of molecules from the pore space depending on their size. No adsorption takes place.



Table 2 gives an overview of the main chromatography types:

**Table 2: Overview of chromatography types**

<b>Type of chromatography</b>	<b>Adsorption principle</b>	<b>Separation principle</b>
Ion exchange chromatography (IEX)	Ionic binding	Surface charge
Hydrophobic interaction chromatography (HIC)	Hydrophobic complex formation	Hydrophobicity
Affinity chromatography	Bio specific interaction	Molecular structure
Reversed phase chromatography (RPC)	Hydrophobic complex formation	Hydrophobicity
Metal chelate chromatography (MCC)	Coordination complex with transition metals	Efficiency of complex formation
Gel filtration (GF) / Size exclusion chromatography (SEC)	Size exclusion	Molecular size and shape
Adsorption chromatography	Surface binding	Molecular structure
Mixed mode chromatography	Several	Several

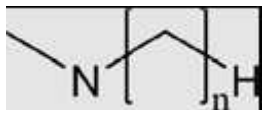
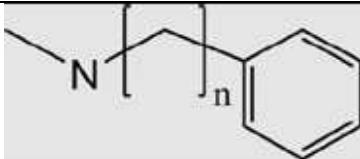
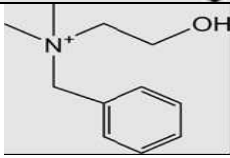
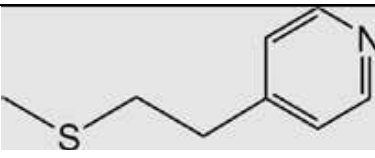

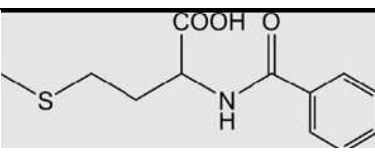
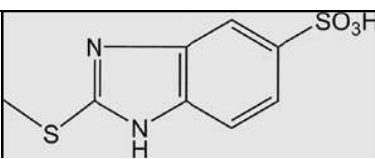
### ***3.2.2 Mixed Mode Chromatography***

The term mixed-mode chromatography is used if a chromatographic sorbent utilizes more than one form of interaction between the stationary phase and the solutes in a feed stream [G. Zhao et al., 2009]. Indeed mixed-mode mechanisms may be involved in every chromatographic separation due to the fact that protein interaction with ligand, linker and matrix consists of more than one adsorption principle. The term mixed-mode only is typically used for resins designed with multi-modal operating ligands [M. Rios, 2007; P. Gagnon et al., 2009].

Compared with other types of chromatography, the benefits of mixed-mode chromatography are its adsorption at high salt concentrations and unique selectivity. Usually these ligands have an aliphatic or aromatic group as the hydrophobic component and an amino, carboxyl or sulfonic group as the ionic moiety, also hydrogen bonding groups have an influences on the performance of mixed-mode adsorbents. These leads to the disadvantage of mixed- mode resins: more often than not the development of a screening method and its optimization needs more effort in development also using statistical experimental approaches – like Design of Experiments [G. Zhao, 2009].

Table 3 gives a short overview of mixed-mode ligands and their resins. The underlined sorbents have been used in this experimental work.

**Table 3: Brief overview of mixed mode resins**

	Name	Structure	Resin
Ligands with positive charge	Alkylamine		<u>HEA Hypercel</u> (Pall Lifescience, NY, USA). (n=8)
	Phenylalkylamine		<u>PPA Hypercel</u> (Pall Lifescience, NY, USA) (n=4)
	N-Benzyl-N-methyl ethanol amine		Capto™ adhere (GE Healthcare, NJ, USA).
	4-Mercaptoethylpyridine		<u>MEP Hypercel</u> (Pall Lifescience, NY, USA).
Ligands with negative charge	Aminoalkyl carboxyl acid		
	2-Benzamido-4-mercaptobutanoic acid		<u>Capto™ MMC</u> (GE Healthcare, NJ, USA).
	2-Mercapto-5-benzimidazole sulfonic acid		<u>MBI Hypercel</u> (Pall Lifescience, NY, USA)

### **3.3 Design of Experiments - DoE**

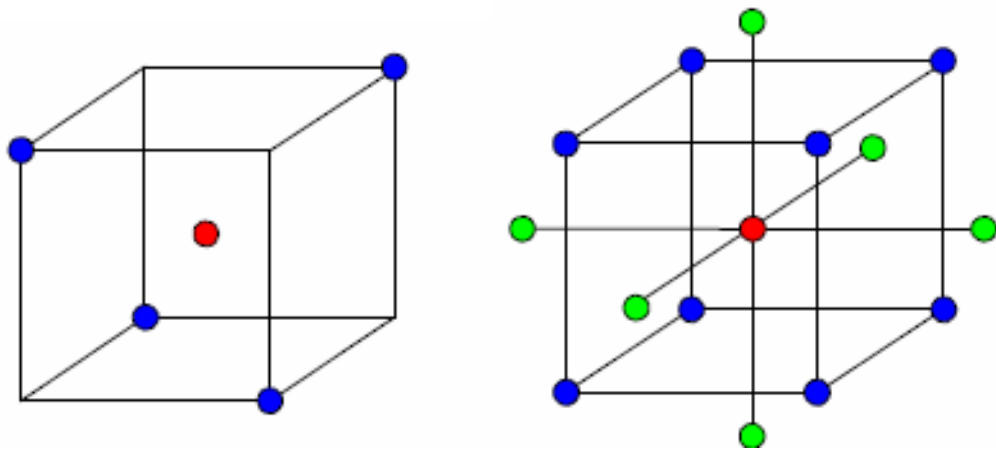
If there are more than one factor that has to be investigated, varying one while leaving the other factor fixed can yield good results, but for optimization it is not the best way to success. This “one factor at a time method” can lead to misinterpretations if factors are not independent from each other. For this, Design of Experiments (DoE) is a methodology for planning experiments, analyzing the results and defining the optimum. Its purpose is the identification and understanding of correlations between defined input variables and the resulting responses to gain the maximum amount of information from the analysis of the experiments while keeping complexity and effort low [S. Soravia and A. Orth, 2006].

This statistical concept is based on the book “Design of Experiments” published by Sir Ronald Aylmer Fisher in 1935 and his statistical experimental design methods he established in the 1920s [R. A. Fisher, 1966]. The principles were first used in agricultural science, biology and medicine and essential innovations like blocking, randomization, and replication originate from his work. His methodology was further characterized by the implementation of analysis of variance which enabled efficient processing of obtained data. In the 1950s DoE was integrated into Japanese industry, in particular by the methods of Taguchi, and later on it was promoted by the advances in electronic data processing [G. Taguchi, 1987].

Depending on the required resolution, the time and effort that are available, different DoE models are used. The full factorial design is the most complex and extensive. When two levels of settings (lower (-) and higher (+) level) are measured, this design comprises  $2^n$  experiments with n representing the number of factors involved. It is the most used design but over  $2^4$  this full factorial design leads to a disproportional high expenditure of work with more information than is generally needed. This leads to a reduction of the model to a fractional factorial design, which reduces effort cost and time but has to be considered carefully since simplification is done on the expense of resolution and significance [S. Soravia and A. Orth, 2006; W. Kleppmann, 1998].

Analysis of Variance (ANOVA) is used to assess the quality of calculated models and is based on an estimation of the natural variability which is achieved by replication of the center point.

In the present experimental work a central composite design was processed (Figure 5). Such a design consists of a full factorial approach extended by centre points and star points.



**Figure 5: Scheme of a  $2^3$  fractional factorial design plus centre point (left) and a full central composite design (right)**

## ***4 Materials and Methods***

### **4.1 Media**

#### ***4.1.1 Chemicals***

If not stated otherwise, chemicals were purchased from Merck (Darmstadt, Germany) and Sigma-Aldrich (St. Louis, USA).

#### ***4.1.2 Water***

The de-ionized water was obtained by an Ultra Clear water purification system (SG Wasseraufbereitung und Regenerierstation GmbH, Barsbüttel, Germany) and used for all chromatography tasks.

For analytical methods ultrapure water from Milli-Q water purification system (Millipore, Billerica, USA) was obtained.

#### ***4.1.3 Vectors and Organisms***

The respective gene was cloned with *XhoI/ NotI* restriction into the plasmid carrying proprietary AOX1-promoters. The expression of the V<sub>HH</sub> domain antibody was obtained in the host *Pichia pastoris* phenotype *CBS 7435 mut<sup>S</sup>*.

#### ***4.1.4 Model Protein***

V<sub>HH</sub> 3 domain antibody, is a dimer featuring a human serum albumin at the C-terminus with a molecular weight of 95.3 kDa and a theoretical pI of 6.6.

## 4.2 Analytical Methods

### 4.2.1 UV-VIS Spectroscopy

In batch adsorption experiments protein concentration was measured using a Spectronic Genesys6 spectrophotometer (Thermo Fisher Scientific, Waltham, USA). After determining the linear range, the final concentration could be calculated using the extinction coefficient of 84190 L/mol\*cm.

### 4.2.2 LDS-PAGE

Lithium dodecyl sulfate polyacrylamide gel electrophoresis (LDS-PAGE) was used as routine analytical method for protein detection.

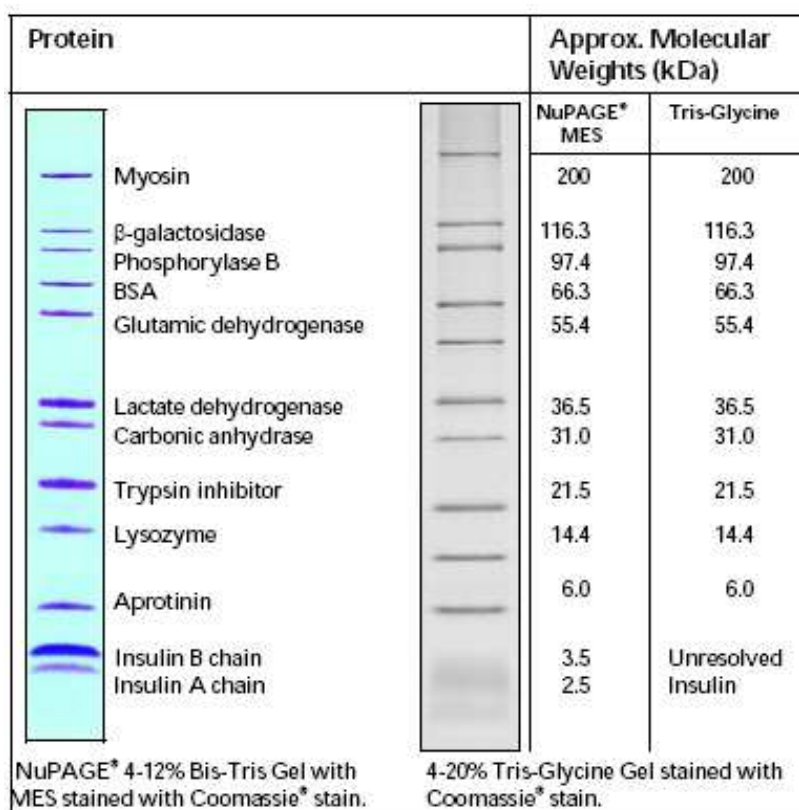


Figure 6: Approximate molecular weight of the protein standard Mark 12 [[http://tools.invitrogen.com/content/sfs/manuals/mark12\\_card.pdf](http://tools.invitrogen.com/content/sfs/manuals/mark12_card.pdf)]

4x LDS sample buffer (Invitrogen, Carlsbad, USA) was mixed with 10%  $\beta$ -mercaptoethanol and diluted into 2x LDS and 1x LDS sample buffer. Samples were diluted with the reduced LDS sample buffer to a concentration of 0.1  $\mu\text{g}/\mu\text{L}$  heated 5 min at 80 °C in an Eppendorf Thermomixer Compact and then centrifuged at 450 rpm in an Eppendorf Mini Spin (Hamburg, Germany). 10  $\mu\text{L}$  per lane were applied to NuPage 12 % Bis-Tris gels (1 mm) and Mark 12 (Figure x) was used as molecular marker (both Invitrogen, Carlsbad, USA). The electrophoresis was carried out in a Novex Mini Cell Chamber filled with 1x MES running buffer (both Invitrogen, Carlsbad, USA) for 50 min with 200 V.

### ***4.2.3 Coomassie Simply Blue Safe Staining***

Staining was carried out using a slightly adapted protocol published by Invitrogen. The gels were fixed for 15 min using the fixating solution outlined in Table 4.

**Table 4: Components fixating solution**

500 mL	EtOH
70 mL	HAc
430 mL	H <sub>2</sub> O

The gels were washed 3 times for 5 min with HQ-H<sub>2</sub>O, then stained for 1 h with Simply Blue Safe Stain (Invitrogen, Carlsbad, USA) and subsequently destained for 1 h with HQ-H<sub>2</sub>O. The stained gels were scanned using a Personal Laser Densitometer SI (Molecular Dynamics, Sunnyvale, USA) and quantified with TotalLab TL120 software.

### ***4.2.4 Silver Staining***

Silver staining was performed using SilverXpress Silver Staining Kit and SilverXpress Silver Staining Protocol for Bis-Tris Gels (Invitrogen, Carlsbad, USA). Stained gels were scanned using a Personal Laser Densitometer SI (Molecular Dynamics, Sunnyvale, USA) but not quantified, because silver gels while appropriate for comparing the purity of a product, cannot be used for quantification.

#### **4.2.5 Protein A - HPLC**

Protein A-High Performance Liquid Chromatography (Protein A-HPLC) was performed using a poros matrix which was operated on an Agilent HPLC station 1100 series (Agilent Technologies, Santa Clara, USA). Elution was performed using a conventional pH-gradient. The absorbance was measured at 214 nm and quantification was performed using the V<sub>HH3</sub> working standard

#### **4.2.6 IEX - HPLC**

Ion-exchange-HPLC (IEX-HPLC) was conducted on an Agilent HPLC station 1100 series (Agilent Technologies, Santa Clara, USA) using a weak cation exchanger column suitable for biomolecules. Samples and standard were diluted to an injection volume with an absolute protein content of 15 µg. Buffer A was a 10 mM phosphate buffer and buffer B a 10 mM phosphate buffer with 1 M NaCl. The column was equilibrated for 1 min, 10 µL of sample was injected and then eluted by gradient elution. The absorbance was measured at 214 nm. All steps were performed at a constant flow rate of 1 mL/min. Protein concentration was determined using the V<sub>HH3</sub> working standard.

#### **4.2.7 SEC - HPLC**

Size-exclusion-HPLC (SEC-HPLC) was performed using a Tosoh 2000 SW (Tosoh Bioscience GmbH, Stuttgart, Germany) column which was operated on an Agilent HPLC station 1100 series (Agilent Technologies, Santa Clara, USA). Samples and standard were diluted to an injection volume with an absolute protein content of 3 µg. For equilibration and elution phosphate buffered saline (PBS)-buffer, pH 7.0 with 5 % isopropyl alcohol (IPA) was used. The column was equilibrated for 1 min, 10 µL of sample was injected and then eluted. All steps were performed at a constant flow rate of 0.3 mL/min. Absorbance was measured at 214 nm protein concentration was quantified using the V<sub>HH3</sub> working standard.



### 4.2.8 RP - HPLC

Reversed-phase-HPLC (RP-HPLC) was conducted on an Agilent HPLC station 1100 series (Agilent Technologies, Santa Clara, USA). For analytical separation a C3 reversed phase matrix with a pore diameter of 300 Å was used. Samples and standard were diluted to an injection volume with an absolute protein content of 1.5 µg. As equilibration buffer A HQ-H<sub>2</sub>O with 0.07 % trifluoroacetic acid (TFA) was used. Elution buffer B contained 0.17 % TFA in acetonitrile (ACN). The column was equilibrated for 1 min, 10 µL of sample was injected and then eluted with a conventional ACN gradient. The absorbance was measured at 214 nm. All steps were performed at a constant flow rate of 0.8 mL/min. Protein concentration was assessed using the V<sub>HH3</sub> working standard.

## 4.3 Fermentation

The fermentation of the secreted V<sub>HH</sub> domain antibody in *Pichia pastoris* was accomplished by the fermentation unit of the BI RCV Process Science as follows:

The seed culture was incubated with YPG medium (Table 5) at 24 °C and 250 rpm for 30 h.

**Table 5: YPG medium for *P. pastoris***

	<b>Component</b>	<b>Amount</b>
1	bacto yeast extract	10 g/L
2	soy peptone	20 g/L
3	glycerol (100 %)	25.2 g/L
4	biotin stock solution	0.1 %

The 20 L main culture was then grown in a defined, adapted basal salt medium with 40 g/L glycerol concentration at pH 6.0 at 24 °C and the pO<sub>2</sub> of 25 % was maintained by increasing the impeller speed from 400 rpm to 1000 rpm and by supplying pure oxygen, as necessary. After 24 h the initial glycerol in the batch medium was exhausted (pO<sub>2</sub> peak) and a short glycerol feed was started to increase biomass. After 27 h of fermentation the feed was switched to methanol to induce protein production.

### **4.3.1 Dry Cell Weight (DCW)**

The dry cell weight (DCW) was determined from 10 mL of fermentation broth. The suspension was centrifuged at 4000 rpm and 4 °C for 15 minutes (Eppendorf 5810R, Germany), washed with deionised water, and again centrifuged at the same conditions. Before drying to a constant weight in an automatic dryer (HG 55 Halogen Moisture Analyzer, Mettler Toledo, Switzerland), the pellet was resuspended in deionised water.

### **4.3.2 Optical Density ( $OD_{550}$ )**

The optical density of the culture broth was measured with a spectral photometer (Spectronic Genesis 5, Spectronic Instruments, USA) at 550 nm. The samples were diluted with OD buffer (Table 6) in order to obtain an absorbance in the linear range between 0.2 and 0.6  $OD_{550}$ . For measuring the blank values, the samples were sterile filtered.

**Table 6: OD Buffer**

<b>Components</b>	<b>Concentration</b>
$Na_2HPO_4 \cdot 12H_2O$	20,73 g/L
$KH_2PO_4$	5,7 g/L
NaCl	11,6 g/L

## **4.4 Primary recovery**

At the end of fermentation the culture broth was centrifuged at 7000 rpm for 30 min using an JLA 10.500 rotor in an Avanti J-26 XP centrifuge (Beckmann Coulter, USA) The supernatant was then filtrated with 1.2  $\mu m$  and 0.65  $\mu m$  using Sartopure 300 filters (Sartorius Stedim Biotech, Aubagne Cedex, France).

## 4.5 Adsorption Isotherms

Equilibrium adsorption isotherms were determined under finite bath conditions (batch uptake experiments). The gel resins – Blue Sepharose 6FF (GE Healthcare, NJ, USA) and Mab Select Xtra (GE Healthcare, NJ, USA) – were washed three times with buffer (50 mM NaAc/50 mM NaCl, pH 5.5) and were subsequently mixed to a 50:50 (gel:buffer) slurry. Protein solutions with various concentrations between 0.1 and 8 mg/ml at an absolute protein content of 5 mg were prepared in 50 mL Greiner tubes, or for the two smallest volumes into 2 mL reaction tubes (see Table 7). 0.1 ml well mixed gel slurry was then added to each protein solutions and incubated for 3 h on an Assistant RM5 roller mixer (Karl Hecht KG, Sondheim/Rhön, Germany). After sedimentation of the gel slurries the protein concentration in the supernatants were determined by UV-VIS spectroscopy

**Table 7: Pipette scheme of adsorption isotherms**

[mg/ml]	Content V <sub>HH 3</sub> [mg]	Slurry [ml]	Stock solution [ml]	50 mM NaAc/50 mM NaCl [ml]	Solution [ml]
0.1	5.000	0.100	1.471	48.429	50.000
0.2	5.000	0.100	1.471	23.429	25.000
0.3	5.000	0.100	1.471	15.096	16.667
0.5	5.000	0.100	1.471	8.429	10.000
1	5.000	0.100	1.471	3.429	5.000
3	5.000	0.100	1.471	0.096	1.667
8*	5.000	0.100	0.319	0.206	0.625

Stock solution=3,4 mg/mL except for \* were different stock solutions were used.

By fitting experimental data to the Langmuir model of adsorption (Equation 1), maximal binding capacities  $q_{max}$  and dissociation constants  $K_D$  were determined:

$$q^* = \frac{q_{max} * c^*}{K_D + c^*} \quad \text{Eq. (1)}$$

where  $q$  is the molecule concentration adsorbed to stationary phase,  $c$  is the soluble molecule concentration in mobile phase,  $q_{max}$  is the maximum binding capacity of the resin and  $K_D = k_d/k_a$ , the dissociation constant of the equilibrium reaction. Superscript \* represents the values when equilibrium is reached.

## 4.6 Chromatography

### 4.6.1 Äkta Chromatography Station

All experimental work including capture, intermediate and alternative purification steps of purification and alternatives therefore were carried out on an Äkta explorer chromatography station (Figure 7) which was controlled by the Unicorn software 5.01 (both GE Healthcare, Uppsala, Sweden). Table 8 shows the components used by the Äkta explorer chromatography station.



**Figure 7: Äkta explorer chromatography station**  
[[www.gelifesciences.com/aptrix/upp01077.nsf/Content/aktadesign\\_platform~akta\\_explorer](http://www.gelifesciences.com/aptrix/upp01077.nsf/Content/aktadesign_platform~akta_explorer)]

**Table 8: Components of Äkta explorer**

<b>Äkta explorer</b>	
UV Detector	Monitor UV900
pump	P-901
UV-Monitor	pH/C-900
Tools Module	box 900 (Controller CU-900)

Equation two and equation three represent yield and purity calculations which were applied for all downstream steps.

$$Yield = \frac{m_{pool}}{m_{load}} * 100\% \quad \text{Eq. (2)}$$

where  $m_{pool}$  is the mass in mg of the pooled fractions and  $m_{load}$  the mass in mg of the load.

$$Purity = \frac{purity_{lane(1)} * \%_{lane(1)}}{100} + \frac{purity_{lane(2)} * \%_{lane(2)}}{100} + \dots + \frac{purity_{lane(n)} * \%_{lane(n)}}{100} \quad \text{Eq. (3)}$$

where  $\%_{lane}$  means the percentage of the fraction of the pooled lanes.

#### **4.6.2 Column Packing**

Columns were packed according to the manufacturers packing recommendations, except for smaller columns with less than about 10 mL. These were packed using a more general procedure:

Column filters were flushed with 20 % EtOH to eliminate air from the column. The bottom adaptor was attached to the column and approximately 1 cm of 20 % EtOH was filled into the column through the bottom outlet. The gel was gently mixed to a homogenous slurry and then poured carefully in a continuous flow into the column. After sufficient sedimentation the upper outlet was also flushed with 20 % EtOH and the column was carefully closed, making

sure that no air bubbles were trapped in the column. After connecting the column to the Äkta explorer system, it was flow packed with the required equilibrium buffer. The packing procedure was performed by applying a defined pressure or alternatively at ~ 120 % of the maximum process flow rate.

### ***4.6.3 Column Evaluation***

In order to evaluate the column performance, the column was equilibrated with 0.2 M NaCl. Then 0.2 column volumes (CV) of 2 M NaCl were injected and eluted with the equilibration buffer. By measuring the retention time and the shape of the salt peak (conductivity profile), the theoretical number of plates per meter (N/m) and the asymmetry factors were calculated by the Unicorn software. The asymmetry factor describes the peak shape and therefore assesses the flow properties of the column. The theoretical plates per meter is a dimensionless number that correlates with the theoretical numbers of equilibria of a substance between the stationary and the mobile phase based on the presumption of a Gaussian peak shape [A. Talamona, 2005].

## 5 Objectives

The aim of the present work was to generate an appropriate downstream process for the purification of the domain antibody  $V_{HH3}$ , a dimer with HSA at the C-terminus, as well as to determine engineering parameters ( $DBC$  10%,  $q_{max}$ ,  $K_D$ ) of the different affinity media that were considered for capture step. Based on the fact that the target protein consists a HSA-tag and a protein-A binding site, both affinity-binding opportunities will be tested with Blue Sepharose 6FF and Mimetic Blue SA HL as HSA-affinity resin and MabSelect Xtra as protein-A affinity resin. With this parameters it would be possible to compare the efficiency of purification for the utilized antibody fragment. Another objective is to study the characteristics of mixed-mode resins for the purification of  $V_{HH3}$ , due to the fact that these resins allow protein binding at high salt concentrations, opening the possibility to utilize this alternative sorbents without prior desalting step.

## 6 Results and Discussion

### 6.1 Clone Screening

The production strain was chosen after screening of >1000 clones in deep well plates. The best 16 clones were selected for re-screening and stability tests were accomplished. Table 9 shows the results of the best three clones with product titers measured by protein-A-HPLC. Clone A was chosen for protein production, because of its high yield and even more important its high stability.

Table 9: Scening results

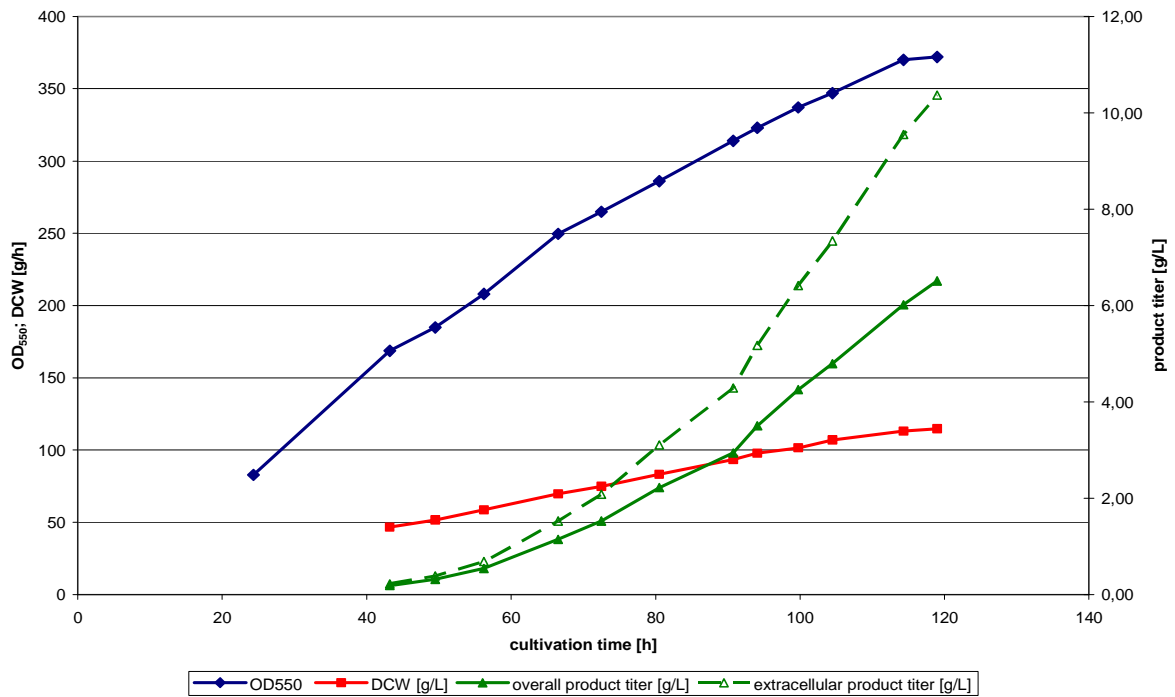
Clone number	A	B	C
Titer [mg/L]	198	205	218
Product Stability [%] (RT / 4°C / -20°C)	100 / 100 / 100	95/100/87	50/100/100

### 6.2 Fermentation

The fermentation process of V<sub>HH3</sub> domain antibody was conducted by the fermentation unit of BI RCV Process Science. A robust process with low feeding rates was chosen for the secreted expression of V<sub>HH3</sub> domain antibody in *Pichia pastoris* exhibiting the following characteristics:

After a phase of 24 h the initial glycerol in the batch medium was exhausted (pO<sub>2</sub> peak) and a short glycerol feed was used to further increase biomass. After 27 h of fermentation the feed was switched to Methanol to induce protein production. The MeOH feed was performed as a ramped linear feed, increasing the feed rates from 20 g/h to 110 g/h within a duration of 92 h. During the fermentation no critical events occurred. The pO<sub>2</sub> could be maintained at 25 % until end of fermentation by increasing the impeller speed up to 1000 rpm and the addition of 0.1 vvm pure oxygen.





**Figure 8: Growth and product formation of V<sub>HH3</sub> domain antibody**

In Figure 8 the results for OD<sub>550</sub>, DCW, titer culture broth and titer supernatant are shown. The growth rates were in the expected range, at the end of fermentation more than 110 g/L dry cell weight were reached. The product titers of 10.5 g/L in the supernatant were very high. However, the high content of biomass in the culture suspension reduces the whole broth titer to ~ 6.5 g/L.

## 6.3 Downstream Process Development

### 6.3.1 Capture Step

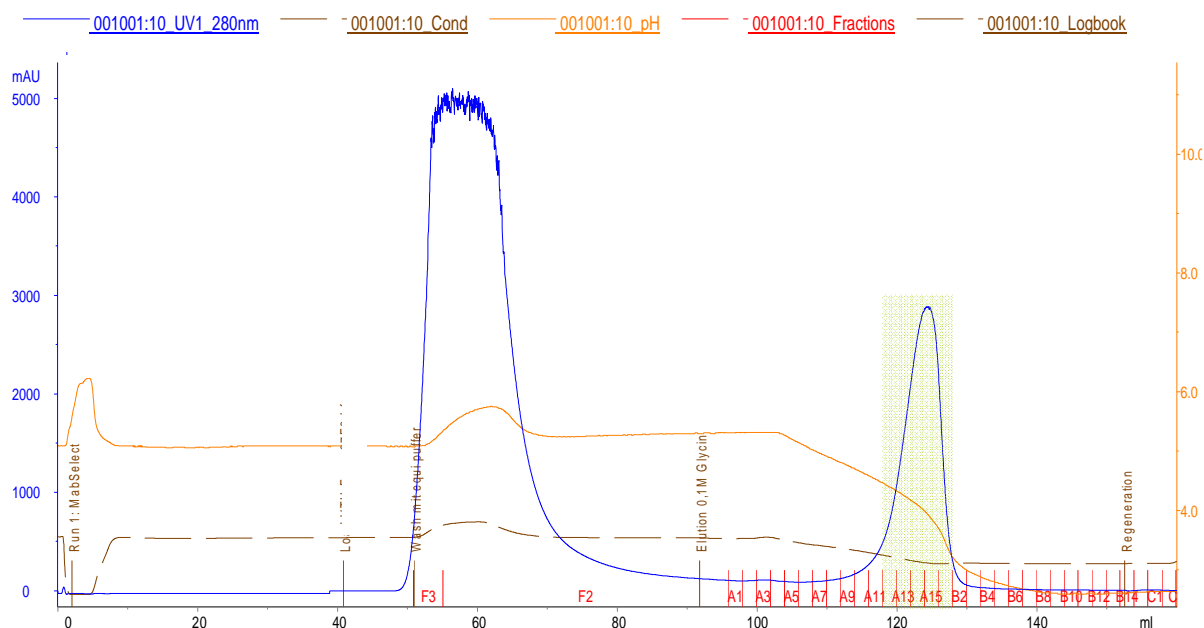
Based on the fact that the target protein consists a HSA-tag and a protein-A binding site, both affinity-binding options were tested. The tested resins were Cibaron Blue 3G media (known as ideal affinity counterpart for albumin) such as Blue Sepharose 6FF (GE Healthcare, NJ, USA) and Mimetic Blue SA HL (ProMetic BioSciences Ltd., Cambridge, UK) and as a Protein-A resin MabSelect Xtra (GE Healthcare, NJ, USA). For the capture step screening all elution fractions were pooled in order to calculate the yield.

#### 6.3.1.1 MabSelect Xtra

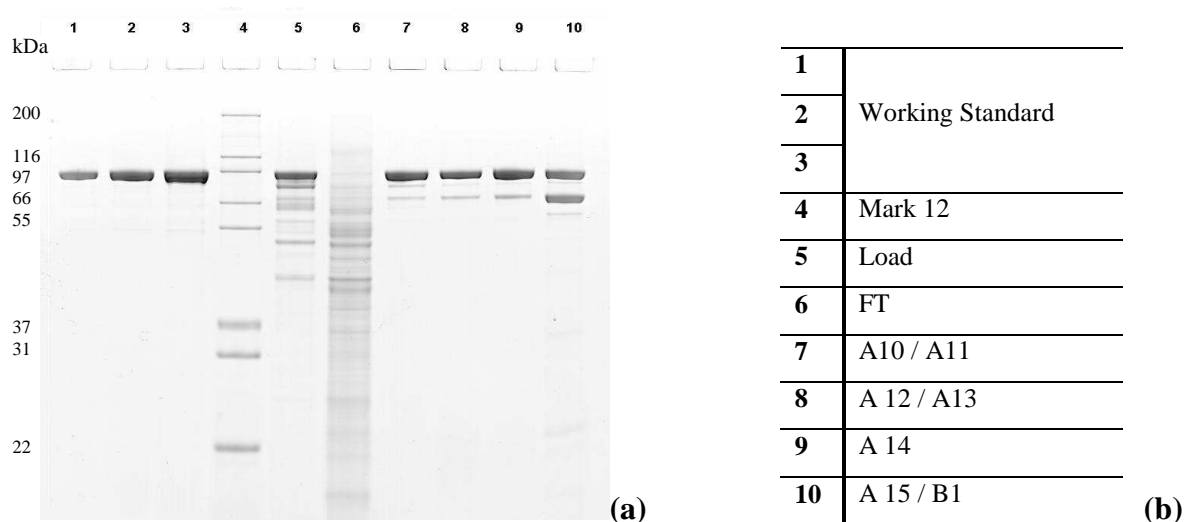
The clone chosen after fermentation evaluation (clone A) and also three others (clone B, C, D) were tested using a 4 mL (51 x 10 mm and 115 x 7 mm respectively) column. Table 10 outlines the method characteristics of the MabSelect Xtra runs with corresponding chromatogram and LDS-PAGE in Figure 9 and Figure 10. Filtrated fermentation supernatant (pH 5.5-6,  $\sigma$  11 – 20 mS/cm) was loaded in each trial. Elution was performed as gradient elution from 0 to 100 % of elution buffer within 10 CV. Load, flow through (FT) and elution fractions were analyzed by LDS-PAGE except the replication run of strain A, which was analyzed by CIEX-HPLC (Table 11).

**Table 10: Method characteristics of MabSelect Xtra capture step**

<b>Step</b>	<b>Buffer</b>	<b>Volume</b>	<b>Linear flow rate [cm/h]</b>
<b>Equilibration</b>	50 mM NaAc / 50 mM NaCl, pH 5.5	10 CV	200
<b>Load</b>	pH 5.5 - 6, $\sigma$ 11 – 20 mS/cm	10 / 20 mL	100
<b>Wash</b>	50 mM NaAc / 50 mM NaCl, pH 5.5	10 CV	100
<b>Elution</b>	0.1 M Glycin, pH 2.5	10 CV	150
<b>Regeneration</b>	0.5 M NaOH	3 CV	50



**Figure 9: Representative chromatogram of MabSelect Xtra run: Fractions pooled from A12-B1**



**Figure 10: Corresponding LDS-PAGE (a) of MabSelect Xtra run with label (b)**

**Table 11: Results of MabSelect Xtra runs**

Clone	Purity [%]	Yield [%]	Method
A	73.5	79.2	LDS-PAGE
A	56.2	49.4	CIEX-HPLC
B	70.8	38.7	LDS-PAGE
C	39.2	16.6	
D	49.2	26.7	

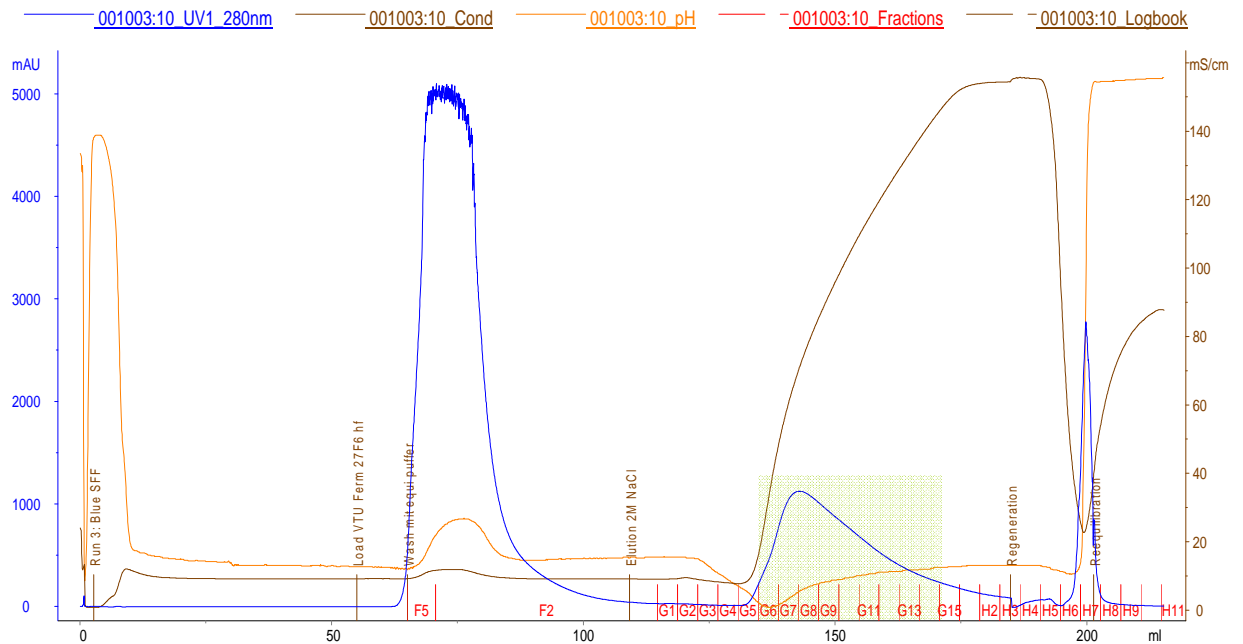
Table 11 summarizes yield and purity values of all performed MabSelect Xtra runs. The values that were calculated on the basis of different analytical methods show purities and yields in a wide spreading range. This could be caused by analytical problems of the applied analyzing methods. The methods are not optimized and showed particularly in the beginning phase of the study variations. As well the measurement of product by LDS-PAGE in the fermentation supernatant was not very accurate, because of the influencing fermentation broth composition. Another reason possible was that the tested clones possessed slightly different properties as they were fermented at different pH values. The different fermentation conditions maybe led to a different isoform pattern with varying binding properties on the resin.

### 6.3.1.2 Blue Sepharose 6FF

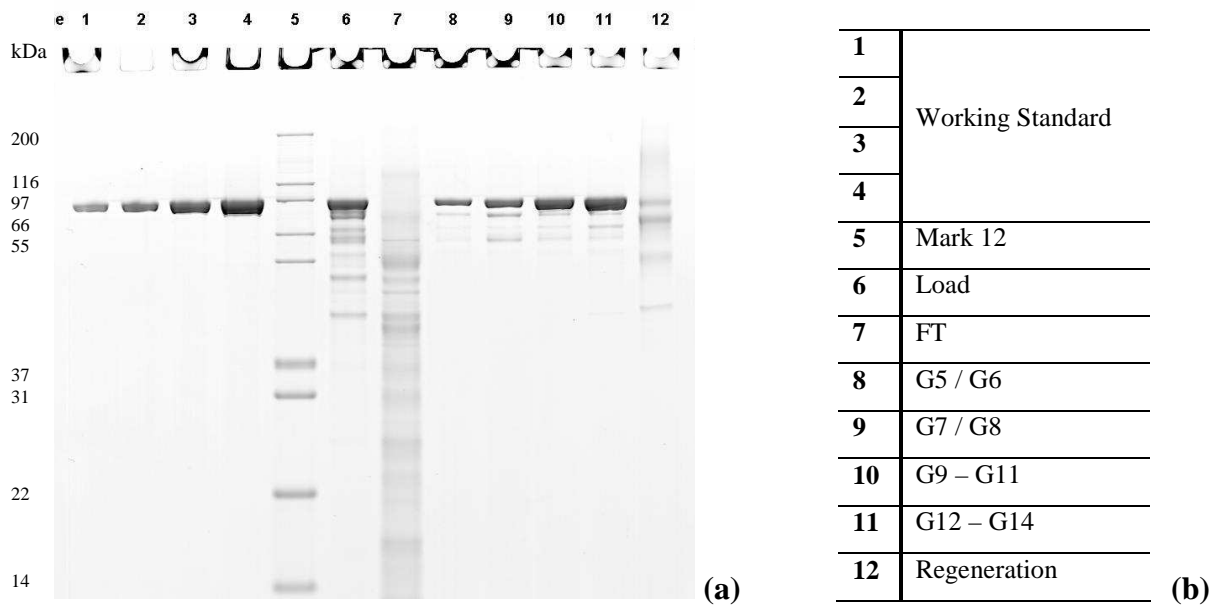
Clone A, B and D were tested using a 5.5 mL (70 x 10 mm) column. The method characteristics are shown in Table 12. Filtrated fermentation supernatant (pH 5.5-6,  $\sigma$  11 – 20 mS/cm) was loaded in each run. Gradient elution was performed, from 0 to 100 % elution buffer within 10 CV. In Figure 11 the chromatogram of the Blue Sepharose 6FF run is displayed with corresponding LDS-PAGE in Figure 12. Load, FT and elution fractions were analyzed by LDS-PAGE (Table 13).

**Table 12: Method characteristics of Blue Sepharose 6FF capture step**

<b>Step</b>	<b>Buffer</b>	<b>Volume</b>	<b>Linear flow rate [cm/h]</b>
<b>Equilibration</b>	50 mM NaAc / 50 mM NaCl, pH 5.5	10 CV	200
<b>Load</b>	pH 5.5 - 6, $\sigma$ 11 – 20 mS/cm	10 mL	100
<b>Wash</b>	50 mM NaAc / 50 mM NaCl, pH 5.5	10 CV	100
<b>Elution</b>	50 mM NaAc / 2 M NaCl, pH 5.5	10 CV	150
<b>Regeneration</b>	0.5 M NaOH	3 CV	50



**Figure 11: Representative chromatogram of Blue Sepharose 6FF run: Fractions pooled from G8-G14**



**Figure 12: Corresponding LDS-PAGE (a) of Blue Sepharose 6FF run with label (b)**

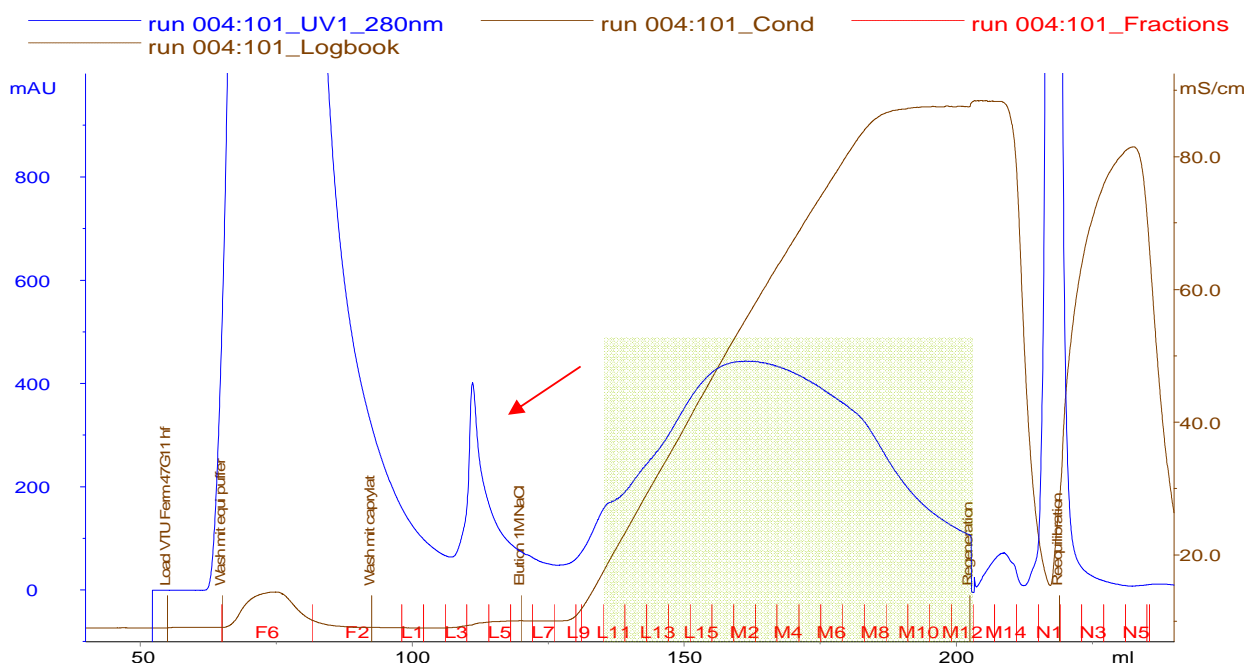
**Table 13: Results Blue Sepharose 6FF runs**

Clone	Purity [%]	Yield [%]	Method
A	83.7	95.2	LDS-PAGE
B	83.7	75.0	
D	92.2	156.2	

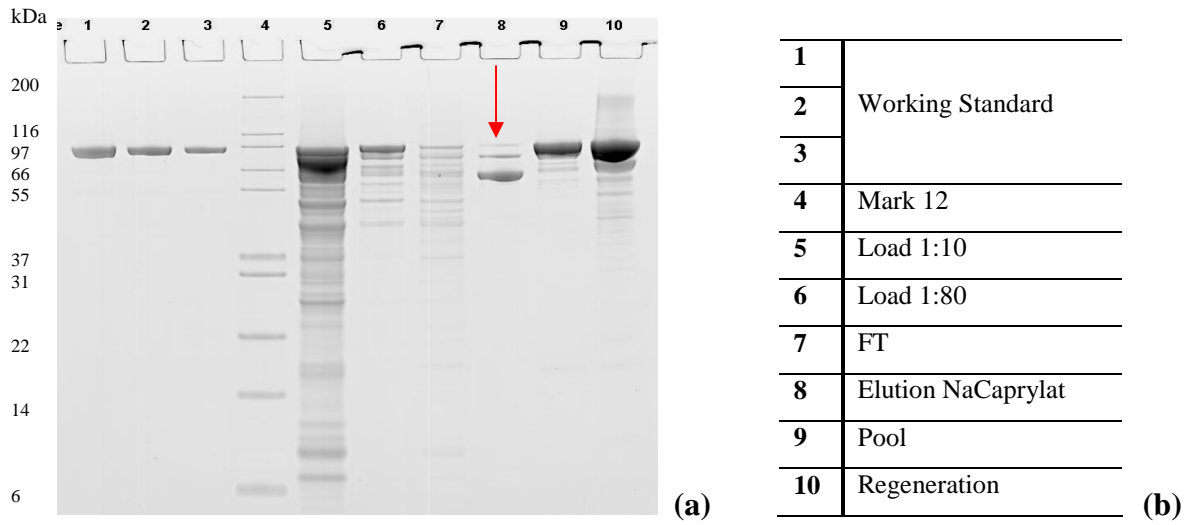
Higher purities and yields were obtained with the Blue Sepharose 6FF resins than with MabSelect Xtra and there was minor variation between results, except one outlier. Representing purification on Blue Sepharose 6FF as more robust process. However both resins showed a second main band (approximately at 70 kDa) in the elution fractions which was defined as possible linker cleavage product. For Blue Sepharose 6FF, experiments demonstrated that this product can be separated by competitive elution (Figure 13 and Figure 14) by using the sodium-salt of caprylic acid (for example sodium octanoate or sodium caprylate) in low concentrations.

**Table 14: Method characteristics of competitive Blue Sepharose 6FF step**

Step	Buffer	Volume	Linear flow rate [cm/h]
<b>Equilibration</b>	50 mM NaAc / 50 mM NaCl, pH 5.5	10 CV	200
<b>Load</b>	pH 5.5 - 6, $\sigma$ 11 – 20 mS/cm	10 mL	100
<b>Wash</b>	50 mM NaAc / 50 mM NaCl, pH 5.5	5 CV	100
<b>Elution 1</b>	50 mM NaAc / 50 mM NaCl, / 25 mM NaCaprylat pH 5.7	5 CV	100
<b>Elution 2</b>	50 mM NaAc / 2 M NaCl	10 CV	150
<b>Regeneration</b>	0.5 M NaOH	3 CV	50



**Figure 13: Chromatogram of Blue Sepharose 6FF, competitive elution using sodium caprylate: Fractions pooled from L11-M12**



**Figure 14: Corresponding LDS-PAGE (a) of competitive Blue Sepharose 6FF run with label (b)**

The method characteristics for competitive elution are shown in Table 14. By reason of the mentioned advantages and because of the lower costs, Blue Sepharose 6FF was chosen as capture step resin.

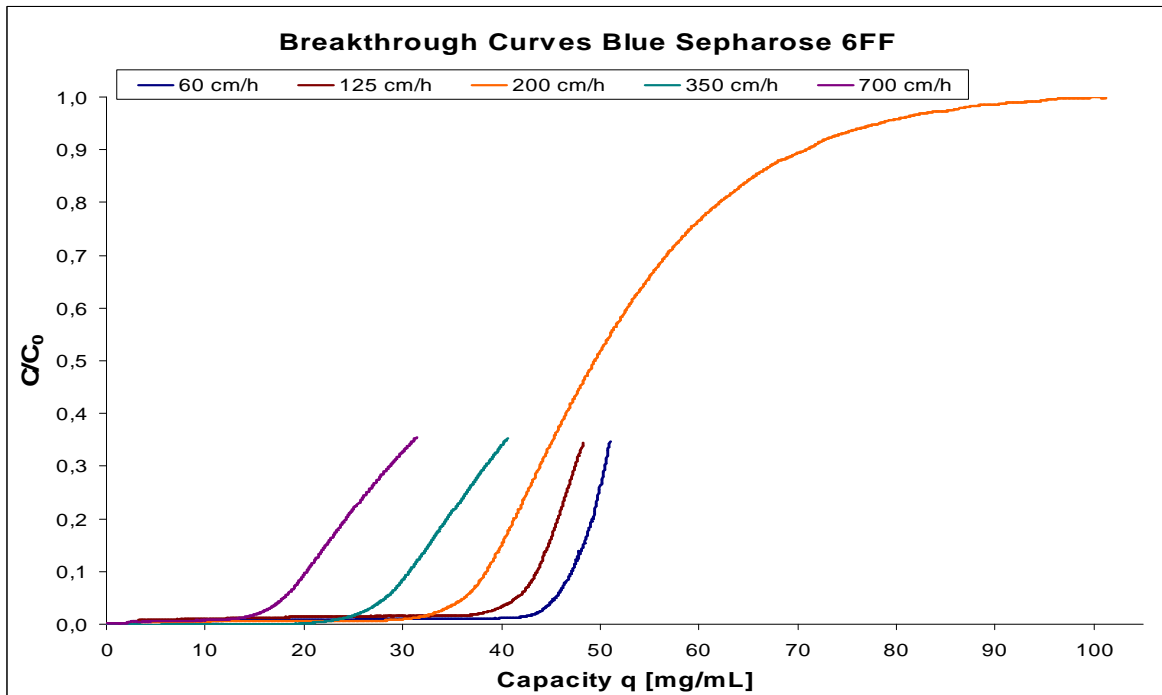
### **6.3.2 Evaluation of Affinity Media**

For confirmation of the selected capture step resin the previous tested affinity media (Blue Sepharose 6FF and MabSelect Xtra) and another HSA-affinity sorbent (Mimetic Blue SA HL) were compared with respect to binding capacities and kinetic parameters. For this purpose dynamic binding capacities at 10 % breakthrough (DBC 10 %) were determined by breakthrough curves. Additionally, adsorption isotherms were performed in order to obtain the maximum equilibrium binding capacities  $q_{max}$  and dissociation constants  $K_D$ .

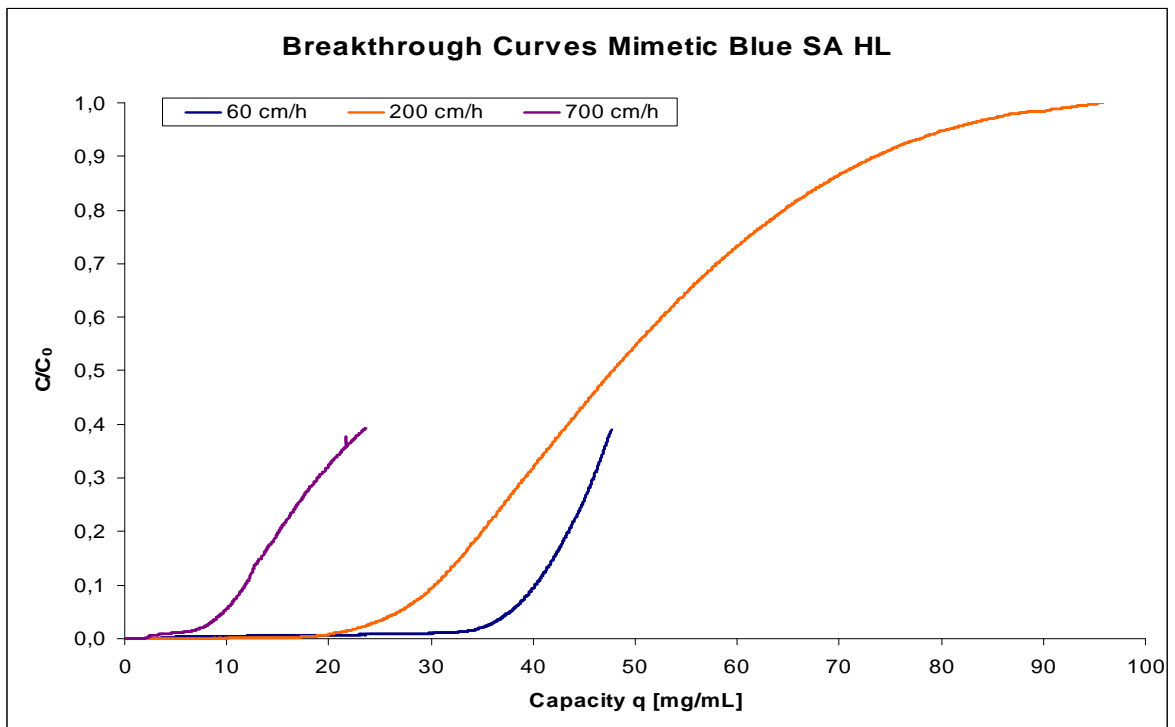
#### **6.3.2.1 Breakthrough Curves**

All experiments were carried out using an Äkta explorer 100 chromatography station. The affinity media were flow packed at a velocity of 800 cm/h to a size of 115 x 6.6 mm that equates a column volume of 3.9 mL. The breakthrough curves were conducted with the same method characteristics as used during capture step. Experiments with Mimetic Blue SA HL were performed identical to experiments with Blue Sepharose 6FF, because this resins are composed out of the same matrix - Sepharose - with the same ligand - Cibaron Blue 3G. The runs were accomplished at different flow velocities (60, 124, 200, 350, 700 cm/h) with a load concentration of 1 mg/mL  $V_{HH3}$ . The load used was already pre-purified by a Blue Sepharose 6FF capture step. Breakthrough profiles of the three affinity media are depicted in Figure 15, Figure 16 and Figure 17. The value for  $C_0$  was obtained from the completed breakthrough curves at 200 cm/h. Because of the limited product, the breakthrough curves were not completed for the other tested velocities and less velocities were tested for MabSelect Xtra and Mimetic Blue SA HL out of the same reason. The breakthrough curves gained for Blue Sepharose 6FF and Mimetic Blue SA HL were very similar and they reached almost the same capacity (visible for 200 cm/h), in contrast to MabSelect Xtra which exhibited a much lower capacity.

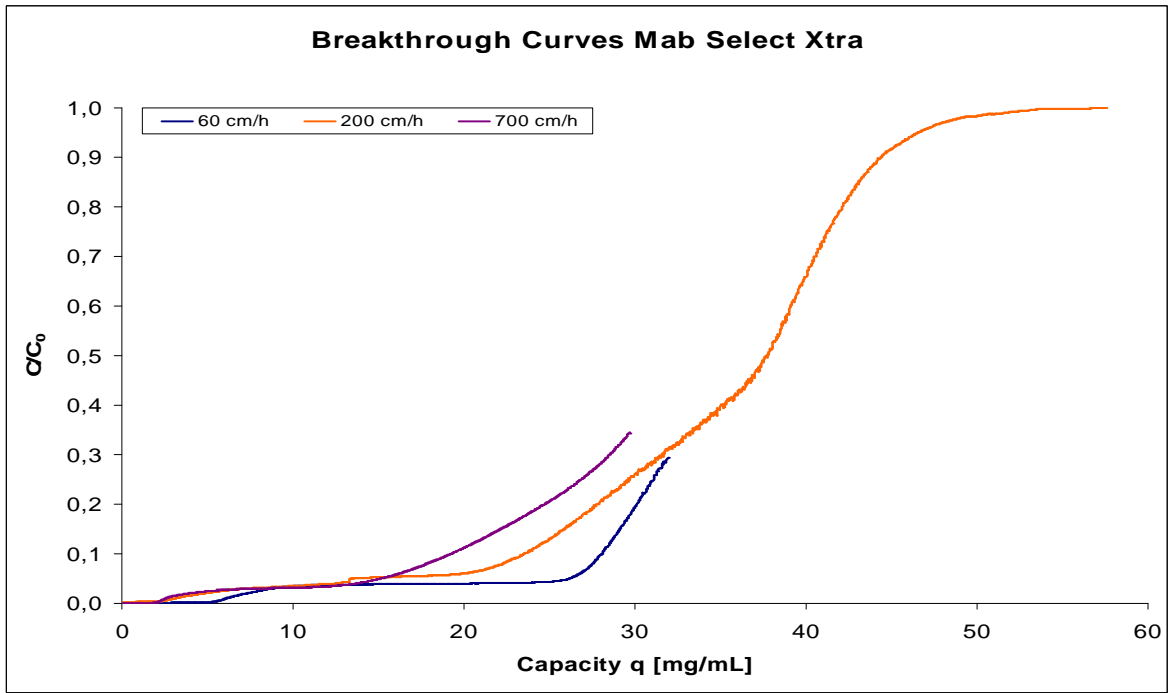




**Figure 15: Breakthrough Curves at different velocities of Blue Sepharose 6FF:** Curves were conducted using pre-purified product



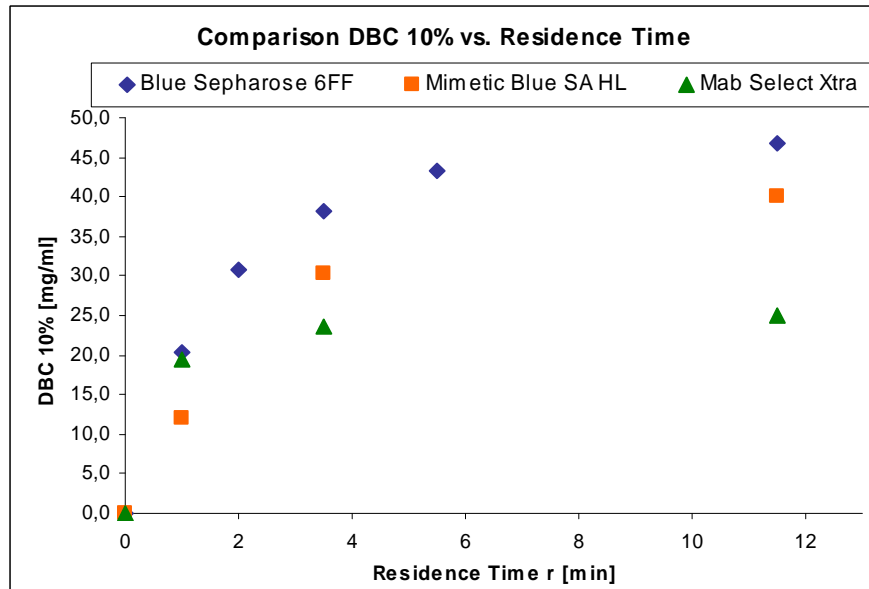
**Figure 16: Breakthrough Curves at different velocities of Mimetic Blue SA HL:** Curves were conducted using pre-purified product



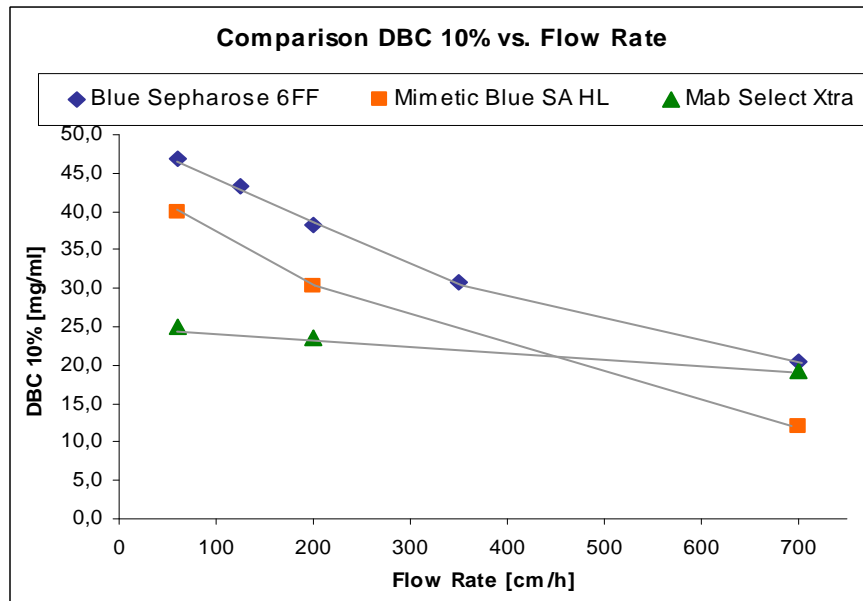
**Figure 17: Breakthrough Curves at different velocities of MabSelect Xtra:** Curves were conducted using pre-purified product

### 6.3.2.2 Binding Capacities

The data obtained from the breakthrough curves was used to receive the values for DBC at 10%. The dependency to residence time and velocity is illustrated in Figure 18 and Figure 19.



**Figure 18: Dynamic binding capacity at 10 % breakthrough vs. residence time of Blue Sepharose 6FF, Mimetic Blue SA HL and MabSelect Xtra**



**Figure 19: Dynamic binding capacity at 10 % breakthrough vs. flow rate of Blue Sepharose 6FF, Mimetic Blue SA HL and MabSelect Xtra**

**Table 15: Comparison of the dynamic binding capacity at 10 % breakthrough**

Flow Rate [cm/h]	Residence Time [min]	DBC 10 % [mg/mL]		
		Blue Sepharose 6FF	Mimetic Blue SA HL	MabSelect Xtra
700	1	20.4	12.0	19.3
350	2	30.8		
200	3.5	38.2	30.3	23.7
125	5.5	43.3		
60	11.5	46.8	39.9	24.9

The decrease of DBC 10 % was almost linear with the increase of the flow rate. For the two HSA-affinity resins the slopes were similar, besides that Mimetic Blue SA HL had a lower DBC 10 % at all velocities. Blue Sepharose 6FF exhibited with 38.2 mg/mL the highest capacity at 200 cm/h compared to Mimetic Blue SA HL with 30.3 mg/mL and MabSelect Xtra with 23.7 mg/mL. At residence times greater than 5.5 min the DBC 10 % reached the equilibrium binding capacity. With an exceeding residence time only marginal gain in capacity would be achieved, resulting in a serious loss of productivity. The decrease of DBC 10 % with increasing flow velocity for MabSelect Xtra was less steep than for the other two resins indicating a faster mass transport. Already a residence time of about 3.5 min gave

reasonable values of DBC 10 % (23.7 mg/mL). This results were not much higher than DBC 10 % of Blue Sepharose 6FF at residence times of around 1 min (20.4 mg/mL). The obtained data confirmed the decision of Blue Sepharose 6FF as sorbent for capture step. An overview of the obtained values is presented in Table 15. All data discussed was gained from experiments with pre-purified product. Because the resins tested are used for capture step, it was important to gain data also with non-purified product. For this purpose breakthrough was investigated with filtrated fermentation supernatant at flow rates of 200 cm/h that corresponded to a residence time of 3.5 min. The calculation of capacity was made for purified and non-purified product by analyzing the pooled product peak with CIEX-HPLC. Identical method characteristics like for breakthrough curves with pre-purified product were used. For determining the amount of load, the DBC 10 % values for each resin were used and an amount of 15 % was added. In Table 16 a comparison of the results is shown.

**Table 16: Comparison of capacities at 200 cm/h of tested affinity media**

		<b>Blue Sepharose 6FF</b>	<b>Mimetic Blue SA HL</b>	<b>MabSelect Xtra</b>
<b>Pre-purified product</b>	<b>DBC 10 % [mg/mL]</b>	38.2	30.3	23.7
	<b>Capacity q * [mg/mL]</b>	36.9	32.8	24.3
<b>Fermentation supernatant</b>	<b>Capacity q * [mg/mL]</b>	29.2	18.5	20.2

\* calculated from elution peak

The values of DBC 10 % conformed to the ones for capacity considering pre-purified V<sub>HH3</sub> domain antibody. With fermentation supernatant the capacity was much lower, especially for Mimetic Blue SA HL. Reason therefore could be that the fermentation supernatant contains product fragments and by-products. These forms bind to the sorbents and take the binding sides of the resin, but are not calculated in for capacity. Pre-purified load contained almost pure product, already separated from fragments of the caprylat elution and forms in the regenerate, what led to the higher capacities. It seems that the Mimetic Blue SA HL resin, although it has the same ligand as Blue Sepharose 6FF, is not suitable for the V<sub>HH3</sub> purification.

### 6.3.2.3 Adsorption Isotherms

Adsorption isotherms measured for Blue Sepharose 6FF and MabSelect Xtra were accomplished using purified V<sub>HH3</sub> domain antibody with the methods equilibration buffer (50 mM NaAc/50 mM NaCl, pH 5.5) at room temperature. The previous experiments showed that the equilibrium binding capacity is achieved fast, therefore a mixing time of 3 h was chosen to be sure to reach equilibrium conditions. With the data received by UV-VIS spectroscopy  $q_{max}$  and  $K_D$  were calculated by using the Langmuir isotherm model (Eq. (1)).

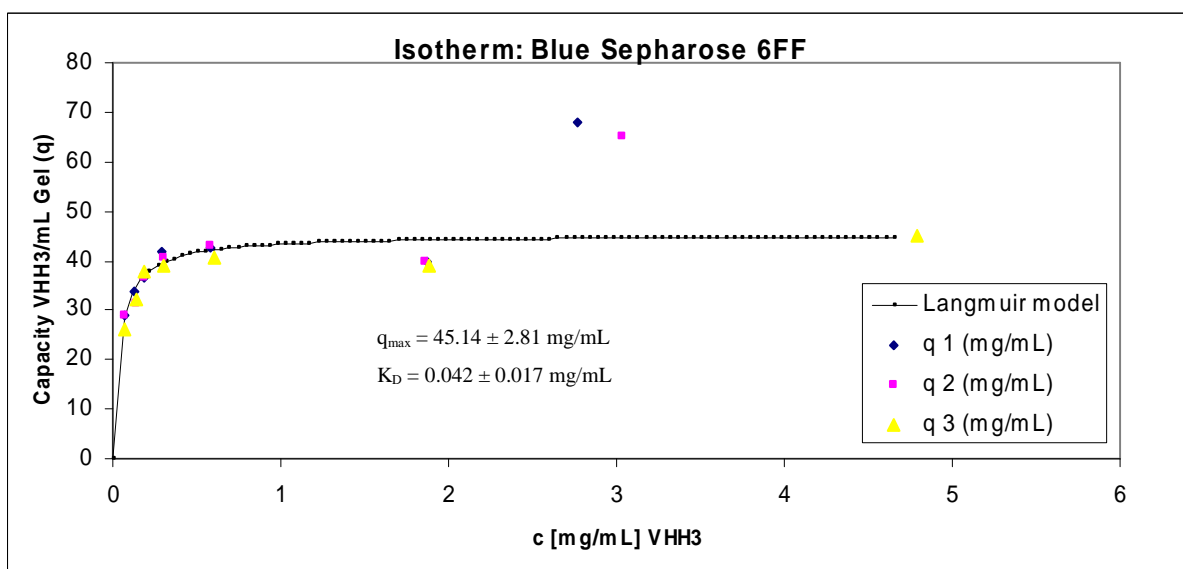


Figure 20: Adsorption Isotherm of Blue Sepharose 6FF

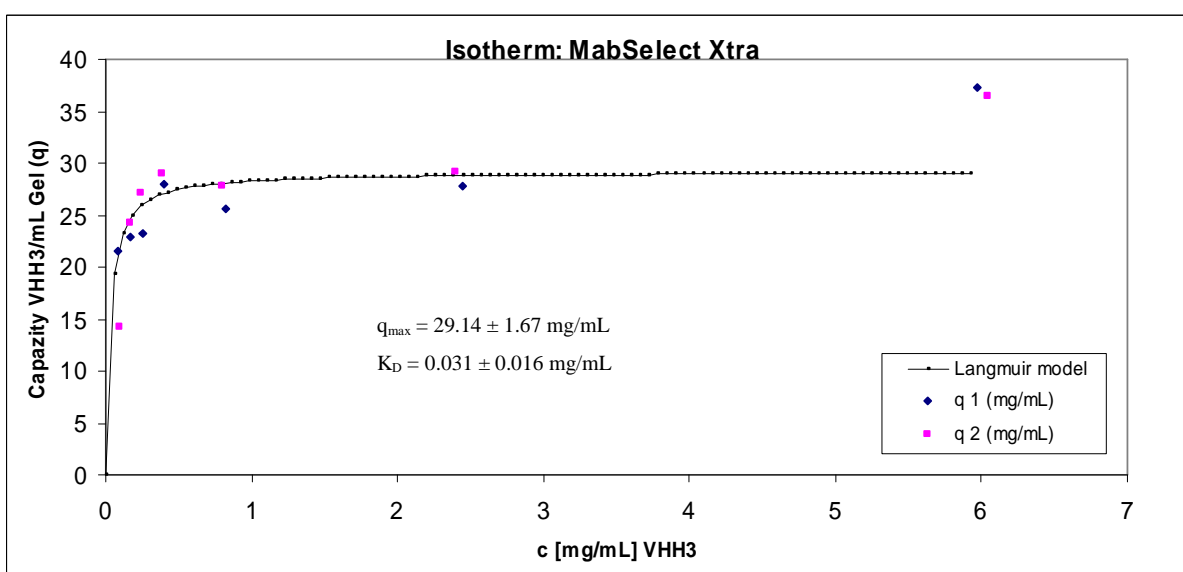


Figure 21: Adsorption Isotherm of MabSelect Xtra

The data gained for the isotherms fitted well to the Langmuir isotherm model (Figure 20 and Figure 21), with both resins showing almost rectangular isotherms.

**Table 17: Summarized engineering parameters of tested affinity media in comparison with data from literature**

	$q_{max}$ [mg/mL]	$K_D$ [mg/mL]	$K_D$ [M]
<b>Blue Sepharose 6FF</b>	$45.14 \pm 2.81$	$0.042 \pm 0.017$	$4.44 E^{-07} \pm 1.79 E^{-07}$
			$1.4 E^{-06} \pm 0.2 E^{-06}$ (a)
			$1.9 E^{-06} \pm 0.4 E^{-06}$ (a)
<b>MabSelect Xtra</b>	$29.14 \pm 1.67$	$0.031 \pm 0.016$	$3.25 E^{-07} \pm 1.68 E^{-07}$
			$5.9 E^{-07} \pm 7.3 E^{-08}$ (b) *

(a) Data from Y. Cui et al., 2003 ( $K_D$  value of HSA molecule on Blue Sepharose 6FF)

(b) Data from R. Hahn et al., 2005 ( $K_D$  value of polyclonal IgG on MabSelect Xtra)

The values for  $q_{max}$  (Table 17) obtained by batch uptake experiments were comparable to the values of DBC 10 % obtained with breakthrough curves at 60 cm/h for both resins. They were 45.14 / 46.8 mg/mL for Blue Sepharose 6FF and 29.14 / 24.9 mg/mL for MabSelect Xtra which is an acceptable range. The variation between the values could arise as well from the fact that  $q_{max}$  was calculated from data measured by UV-VIS spectroscopy and that perhaps for MabSelect Xtra equilibrium conditions were not completely reached at the tested velocity of 60 cm/h (11.5 min residence time). To confirm this, uptake kinetic measurements would be necessary.  $K_D$  value of  $\sim 0.042$  mg/mL or  $\sim 4.44 \times E^{-07}$  M (M.W. of V<sub>HH3</sub>: 95.000 Da) was one magnitude lower than published values of HSA binding on Blue Sepharose 6FF [Y. Cui et al., 2003]. In the referred publication an equilibrium time of just 5 min was used, therefore equilibrium conditions were not reached. The calculated  $K_D$  of MabSelect Xtra resin had the same dimension as the published value of IgG binding on MabSelect Xtra [R. Hahn et al., 2005].

### 6.3.3 Intermediate Step

Different types of chromatography media were tested for intermediate step (Table 18). As starting material Blue Sepharose 6FF pool ( $\sigma$  110-115 mS/cm) and MabSelect Xtra pool ( $\sigma$  10 mS/cm) was used. The amount of product loaded in each run was between 4 and 10 mg product/mL gel. For yield calculation only the elution fractions with higher purities as the loading material (LDS-PAGE) were considered. Loading conditions were chosen in respect to a applicable change from capture to intermediate step.

**Table 18: Gel resins used for intermediate screening**

<b>Strong anion exchanger (AIEX)</b>	Fractogel EMD TMAE (Merck, Darmstadt, Germany)
	Q Sepharose FF (GE Healthcare, Uppsala, Sweden)
<b>Weak anion exchanger (AIEX)</b>	DEAE Sepharose FF (GE Healthcare, Uppsala, Sweden)
<b>Strong cation exchanger (CIEX)</b>	Fractogel EMD SO <sub>3</sub> (Merck, Darmstadt, Germany)
	SP Sepharose HP (GE Healthcare, Uppsala, Sweden)
<b>Weak cation exchanger (CIEX)</b>	CM Sepharose HP (GE Healthcare, Uppsala, Sweden)
<b>Hydrophobic interaction chromatography (HIC)</b>	Phenyl Sepharose HP (GE Healthcare, Uppsala, Sweden)
	Toyopearl Phenyl 600-M (Tosoh Bioscience GmbH, Stuttgart, Germany)

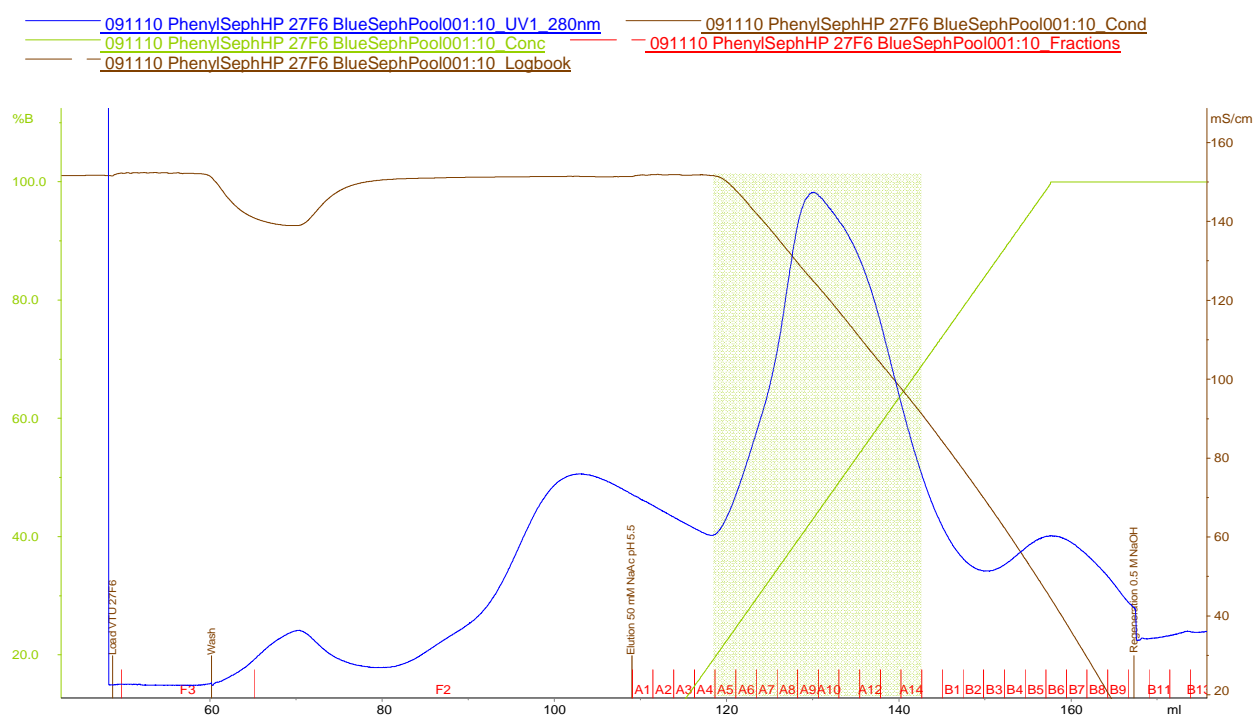
#### 6.3.3.1 HIC - Phenyl Sepharose HP

Method characteristics of Phenyl Sepharose HP are shown in Table 19. Tests were performed with a 4.8 mL (61 x 10 mm) column using Blue Sepharose 6FF pool as loading material. The resin was tested with 1.5 and 2 M NaCl Equilibration buffer with load adjusted to the respective conductivity and a pH of 5.5. The elution gradient was programmed from 0 to 100 % elution buffer in 10 CV, continued by 2 CV at 100 %.

**Table 19: Method characteristics of Phenyl Sepharose HP**

Step	Buffer	Volume	Linear flow rate [cm/h]
Equilibration	50 mM NaAc / 1.5 - 2 M NaCl, pH 5.5	10 CV	300
Load	pH 5.5, $\sigma$ 120 - 145 mS/cm		150
Wash	50 mM NaAc / 2 M NaCl, pH 5.5	5 CV	200
Elution	50 mM NaAc, pH 5.5	12 CV	200
Regeneration	0.5 M NaOH	3 CV	200

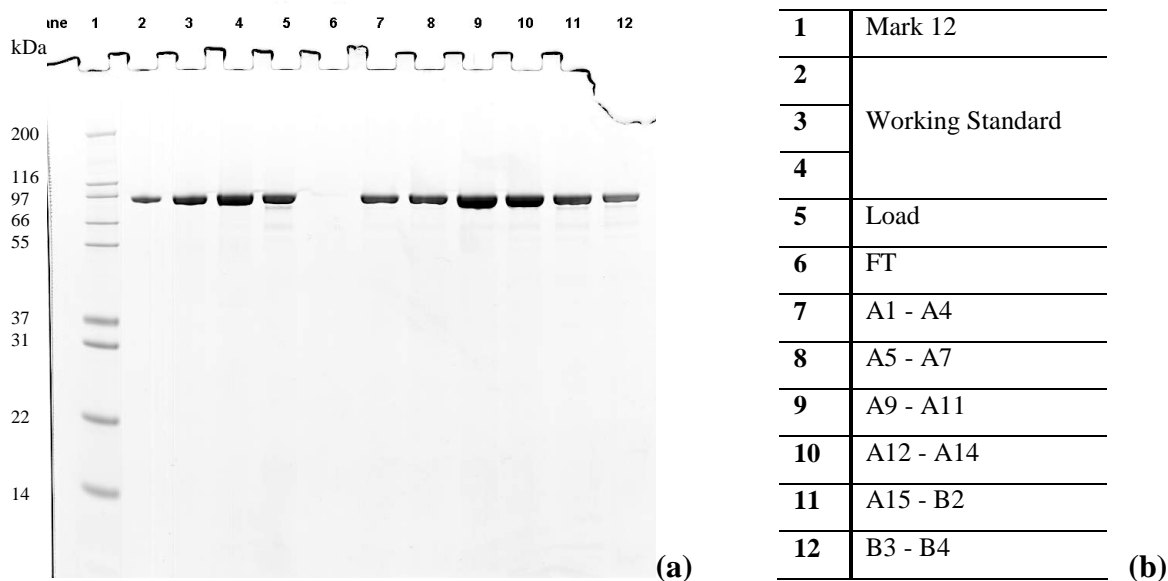
At 2 M NaCl most efficient binding with only little product loss during wash could be observed. Figure 22 and Figure 23 show that the main product elutes already at the beginning of the gradient slope (~ 120 mS; corresponds to ~ 1.5 M NaCl). Therefore, loading at 1.5 M NaCl ended up in too weak binding, resulting in losing most of the product.



**Figure 22: Chromatogram of Phenyl Sepharose HP run with 2 M NaCl equilibration:** Fractions pooled from A5-A14

The Phenyl Sepharose HP resin exhibited low yields (Table 20). At 1.5 M NaCl almost no product could be bound on the resin and also at 2 M NaCl the results were quite poor. Product was found in all fractions together with isoforms.





**Figure 23: Corresponding LDS-PAGE (a) with label (b)**

**Table 20: Results Phenyl Sepharose HP runs**

Run	Purity [%]	Yield [%]	Method
1 – (2 M)	99.3	40.6	LDS-PAGE
2 – (1.5 M)	79.0	3.5	
3 – (2 M)	82.4	14.2	

Run 1 produced great purity with a yield possible to enhance with optimization of the applied method, but run 3, conducted with the same conditions as run 1, could not confirm the expectations and yielded in poor results. Purification by Phenyl Sepharose HP seems to be no robust process.

### 6.3.3.2 HIC – Toyopearl Phenyl 600-M

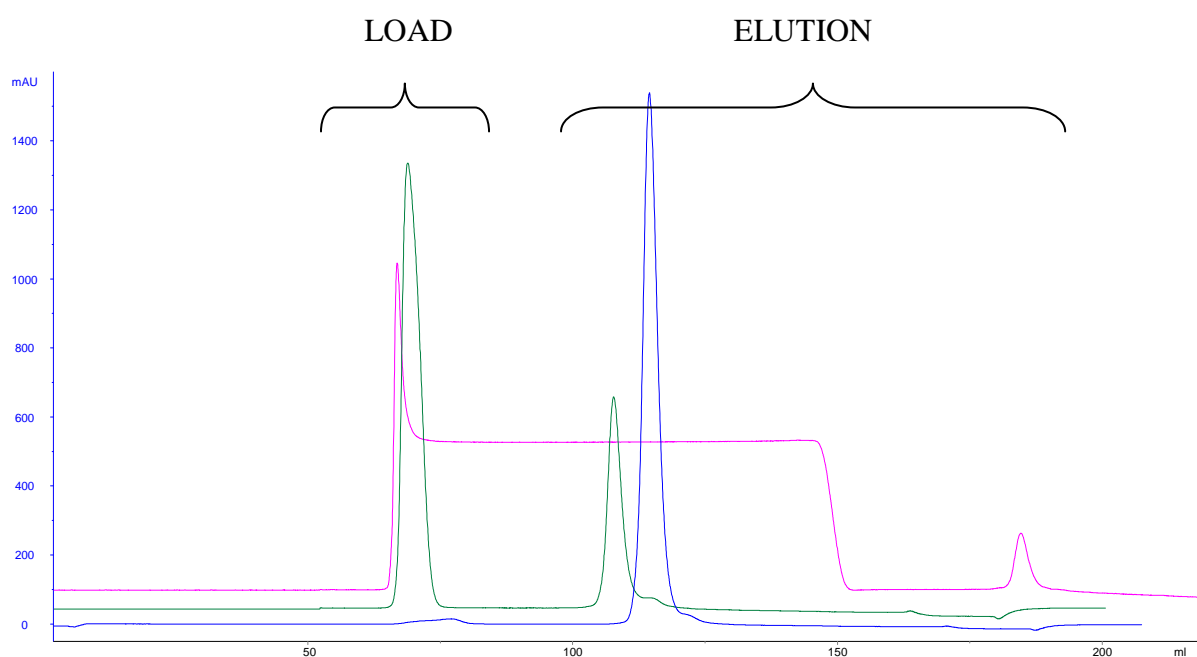
Toyopearl Phenyl 600-M was tested due to characteristics similar to Phenyl Sepharose HP. 3.1 mL ( 39 x 10 mm) columns were tested using Blue Sepharose pool. They were equilibrated with 1.5 M and 2 M NaCl and load was adjusted to the utilized conductivity and pH 5.5. Also same method characteristics as for Phenyl Sepharose HP were applied. Results were comparable with yields around 50 % and purities around 70 %. Also this resin showed low binding at 1.5 M NaCl binding condition.

### 6.3.3.3 AIEX - Fractogel EMD TMAE

In order to test Fractogel EMD TMAE resin, a 5.5 mL (70 x 10 mm) column was used. Different conductivity conditions of Blue Sepharose 6FF load were investigated (Figure 24) and a product amount of 4.5 mg/mL was loaded. For this purpose the load was desalted using Amicon Ultra 10k desalting tubes (Millipore, Billerica, USA) or diluted with equilibration buffer. Since the tested resin was an AIEX resin, pH of the load was adjusted to pH 8.0, in order to be above the pI of 6.6. Table 21 shows the applied method. The elution gradient was programmed from 0 to 100 % elution buffer in 10 CV.

**Table 21: Method characteristics of Fractogel EMD TMAE**

Step	Buffer	Volume	Linear flow rate [cm/h]
<b>Equilibration</b>	20 mM Tris-HCl, pH 8.0	10 CV	300
<b>Load</b>	pH 8.0, $\sigma$ 11 / 26 / 38 mS/cm		150
<b>Wash</b>	20 mM Tris-HCl, pH 8.0	5 CV	200
<b>Elution</b>	50 mM Tris-HCl / 1 M NaCl, pH 8.0	10 CV	200
<b>Regeneration 1</b>	50 mM Tris-HCl / 2 M NaCl, pH 8.0	3 CV	200
<b>Regeneration 2</b>	0.5 M NaOH	3 CV	150



**Figure 24: Comparison of Fractogel EMD TMAE runs – blue: 11 mS/cm; green: 26 mS/cm; pink: 38 mS/cm**

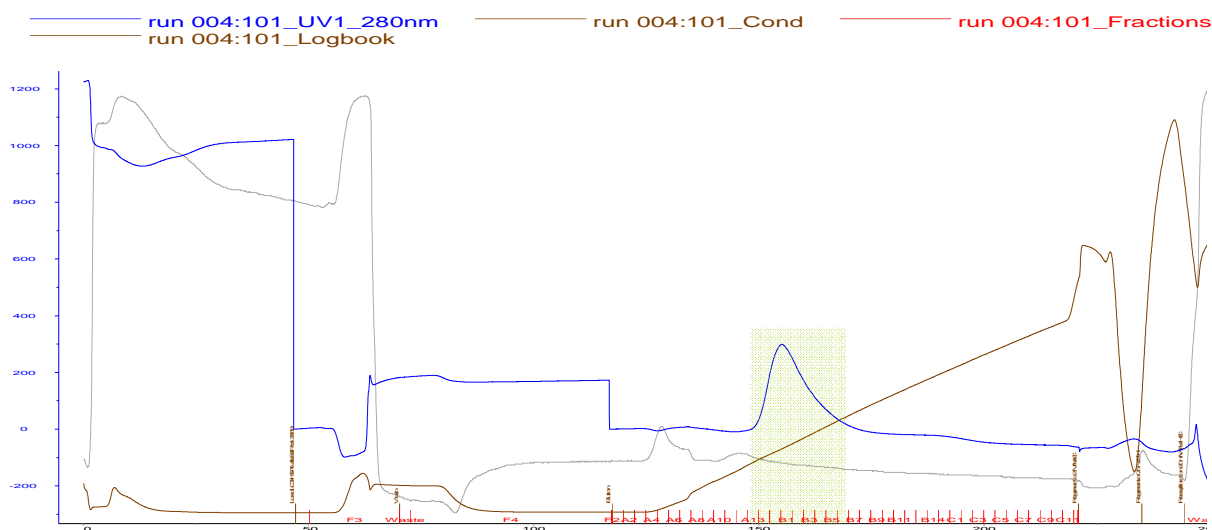
**Table 22: Results Fractogel EMD TMAE runs**

Conductivity $\sigma$ [mS/cm]	Purity [%]	Yield [%]	Method
11	98	47.1	LDS-PAGE
26	100	9.3	
38	89	1.2	

The experiments showed that binding occurs only at rather low conductivities, even though the yield was not very high (Table 22). Anyway, optimization of the method conditions such as even lower loading conductivity, could enhance the gained yield of 47.1 %. At higher conductivities, the main part of the product broke through during loading. Purities of almost 100 % also showed great potential for the use of the Fractogel EMD TMAE resin in purification process of  $V_{HH3}$ .

#### 6.3.3.4 AIEX - Q Sepharose FF

In order to test Q Sepharose FF a 4.7 mL (60 x 10 mm) and a 1.2 mL (62 x 5 mm) column were used. MabSelect Xtra pool was taken as loading material because of its low conductivity (~10 mS/cm). The same method as used for Fractogel EMD TMAE chromatography was used for testing the Q Sepharose FF resin, both being strong AIEX sorbents. Figure 25 shows the chromatogram of one Q Sepharose FF run.



**Figure 25: Chromatogram of Q Sepharose FF run: Fractions pooled from A13-B5**

**Table 23: Result Q Sepharose FF runs**

Run	Purity [%]	Yield [%]	Method
1	77.8	15.1	LDS-PAGE
2	80.2	54.0	

Results (Table 23) ended up in low, fluctuating yields and poor purities. The poor reproducibility indicated that Q Sepharose FF step exhibited no robustness and therefore it was not suitable as intermediate purification step.

### 6.3.3.5 AIEX - DEAE Sepharose FF

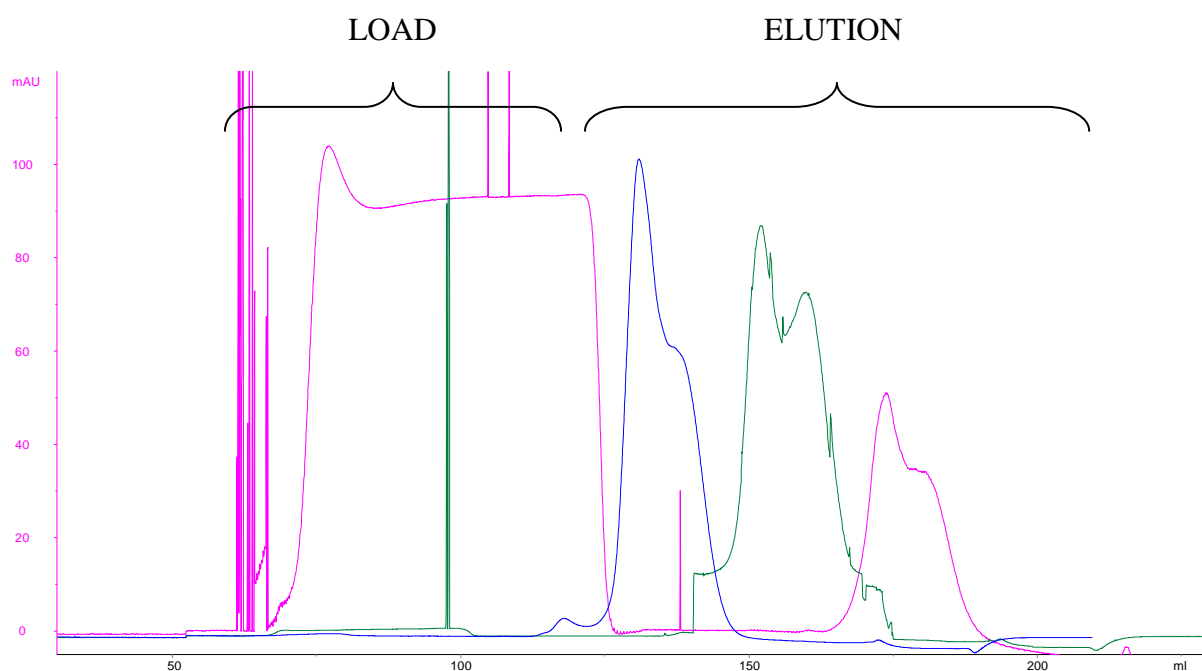
DEAE Sepharose FF - a weak AIEX resin - was tested with a 1.2 mL (65 x 5 mm) column. As load MabSelect Xtra pool was used ( $\sigma$  10 mS/cm). Again, the same method characteristics as used for Fractogel EMD TMAE and Q Sepharose FF were applied. Experiments showed similar results as observed for all AIEX resins. The yield of all AIEX resins was around 50 % or lower and purity was not high enough to accomplish specifications needed for intermediate step, except for Fractogel EMD TMAE.

### 6.3.3.6 CIEX - Fractogel EMD SO<sub>3</sub>

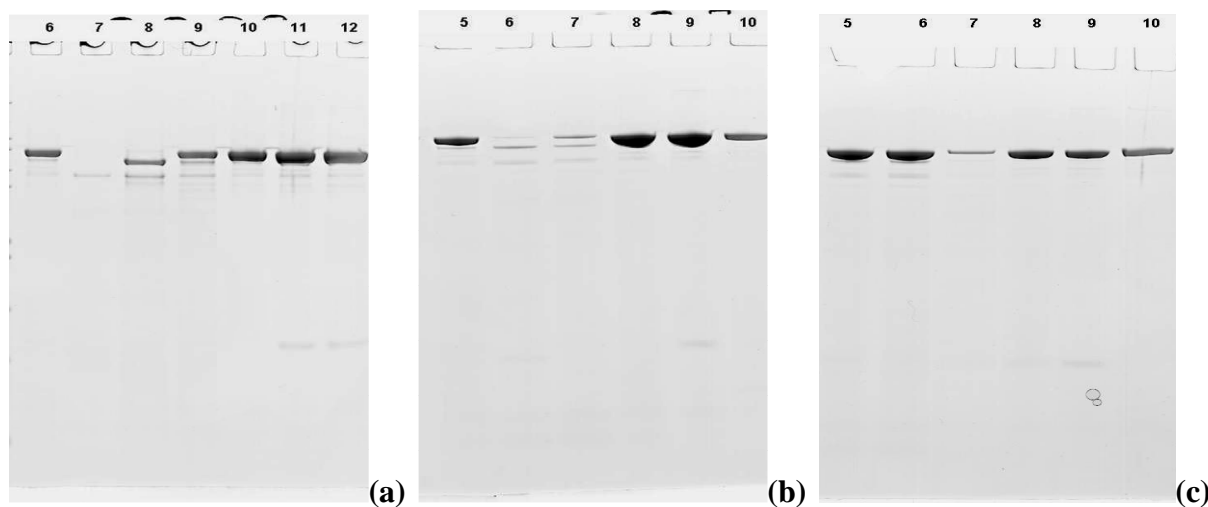
Experiments with Fractogel EMD SO<sub>3</sub> were conducted with a 5.5 mL (70 x 10 mm) column and Blue Sepharose 6FF load with a product amount of 4.5 mg/mL. The load was desalted or diluted with equilibration buffer to test different loading conditions regarding conductivity. Method characteristics are displayed in Table 24. Because the tested resin was a CIEX resin, pH of the load was adjusted to pH 5.5, in order to be below the pI of 6.6. The elution gradient was accomplished from 0 to 50 % elution buffer in 10 CV (elution with 1 M NaCl) continued by 100 % elution buffer for 2 CV (elution with 2 M NaCl). Figure 26 shows the elution peak of the three runs with the different conductivities and corresponding LDS-PAGE (Figure 27, Table 25).

**Table 24: Method characteristics of Fractogel EMD SO<sub>3</sub>**

Step	Buffer	Volume	Linear flow rate [cm/h]
Equilibration	20 mM NaAc, pH 5.5	10 CV	300
Load	pH 5.5, $\sigma$ 9.2 / 25 / 42 mS/cm		150
Wash	20 mM NaAc, pH 5.5	5 CV	200
Elution	50 mM NaAc / 2 M NaCl, pH 5.5	12 CV	200
Regeneration	0.5 M NaOH	3 CV	200



**Figure 26: Comparison of Fractogel EMD SO<sub>3</sub> runs – blue: 9.2 mS/cm; green: 25 mS/cm; pink: 42 mS/cm**



**Figure 27: Corresponding LDS-PAGE Fractogel EMD SO<sub>3</sub>**

**Table 25: Label of Fractogel EMD SO<sub>3</sub> LDS-PAGE**

<b>6</b>	Load	<b>5</b>	Load	<b>5</b>	Load
<b>7</b>	FT	<b>6</b>	FT	<b>6</b>	FT
<b>8</b>	Elution fractions	<b>7</b>	Elution fractions	<b>7</b>	Elution fractions
<b>9</b>		<b>8</b>		<b>8</b>	
<b>10</b>		<b>9</b>		<b>9</b>	
<b>11</b>		<b>10</b>		<b>10</b>	
<b>12</b>					

**Table 26: Results Fractogel EMD SO<sub>3</sub>**

<b>Conductivity <math>\sigma</math> [mS/cm]</b>	<b>Purity [%]</b>	<b>Yield [%]</b>	<b>Method</b>
<b>9.2</b>	94.5	20.5	LDS-PAGE
<b>25</b>	97.7	19.7	
<b>42</b>	95.1	7.0	

Unlike AIEX, protein binding at higher conductivity – up to 25 mS/cm - was observed, nevertheless the product yield was quite low (Table 26). Elution already occurred at 1 M NaCl. Elution fractions were also analyzed by SEC-HPLC - results showed that aggregates occurred in the fractions of the second part of the elution peak. Even high purities of around 95 % were reached, the low yields of around 20 % showed poor potential in optimization, as well as other already tested resins indicated better opportunities in the purification of domain antibody V<sub>HH3</sub>.

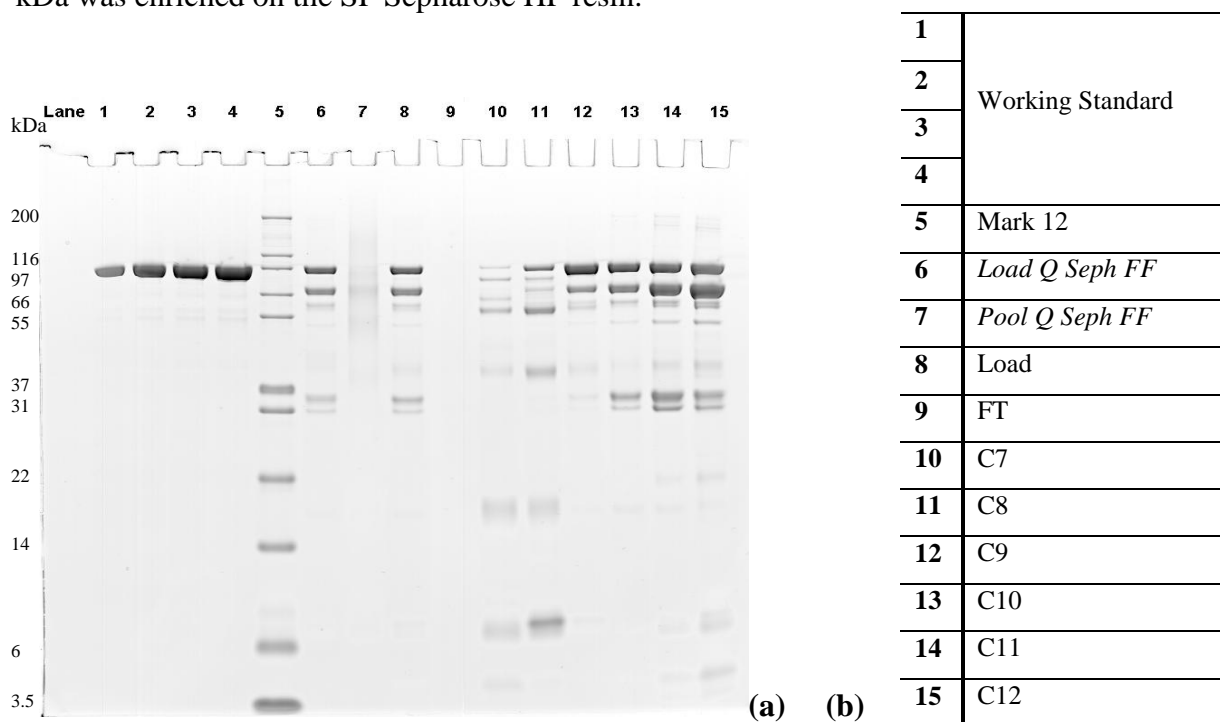
### **6.3.3.7 CIEX - SP Sepharose HP**

In order to test SP Sepharose HP a 4.3 mL (55 x 10 mm) column was used. MabSelect Xtra pool was applied as loading material. Fractogel EMD SO<sub>3</sub> and SP Sepharose SP are both strong CIEX resins, therefore a similar method was utilized. The method characteristics are shown in Table 27. Load was adjusted to pH 5.5. Elution gradient was performed from 0 to 100 % elution buffer in 10 CV with a subsequent hold step at 100 % elution buffer for 2 CV.

**Table 27: Method characteristics of SP Sepharose HP**

Step	Buffer	Volume	Linear flow rate [cm/h]
<b>Equilibration</b>	50 mM NaAc, pH 5.5	10 CV	150
<b>Load</b>	pH 5.5, $\sigma$ 10 mS/cm		80
<b>Wash</b>	50 mM NaAc, pH 5.5	10 CV	150
<b>Elution</b>	50 mM NaAc / 2 M NaCl, pH 5.5	12 CV	100
<b>Regeneration 1</b>	2 M NaCl	3 CV	100
<b>Regeneration 2</b>	0.5 M NaOH	3 CV	100

Elution occurred already at salt concentrations < 1 M NaCl. LDS-PAGE (Figure 28) shows that no significant separation of the two main bands occurred. An additional band at about 37 kDa was enriched on the SP Sepharose HP resin.



**Figure 28: LDS-PAGE of SP Sepharose HP (a) with label (b)**

**Table 28: Results SP Sepharose HP runs**

Run	Purity [%]	Yield [%]	Method
1	65.9	28.5	LDS-PAGE
2	65.5	35.0	

In both SP Sepharose HP runs just one fraction was pure enough to achieve the pooling criterion. Anyway there was almost no improvement in purity using SP Sepharose HP. Almost no separation between by-products, product-fragments and product lane was achieved. Hence the obtained yield was quite low with values of 28.5 % and 35 % (Table 28). The purity could probably be enhanced if Blue Sepharose 6FF pool would be used as load, but similar to the Fractogel EMD SO<sub>3</sub> resin the yield would be still expected to be very low.

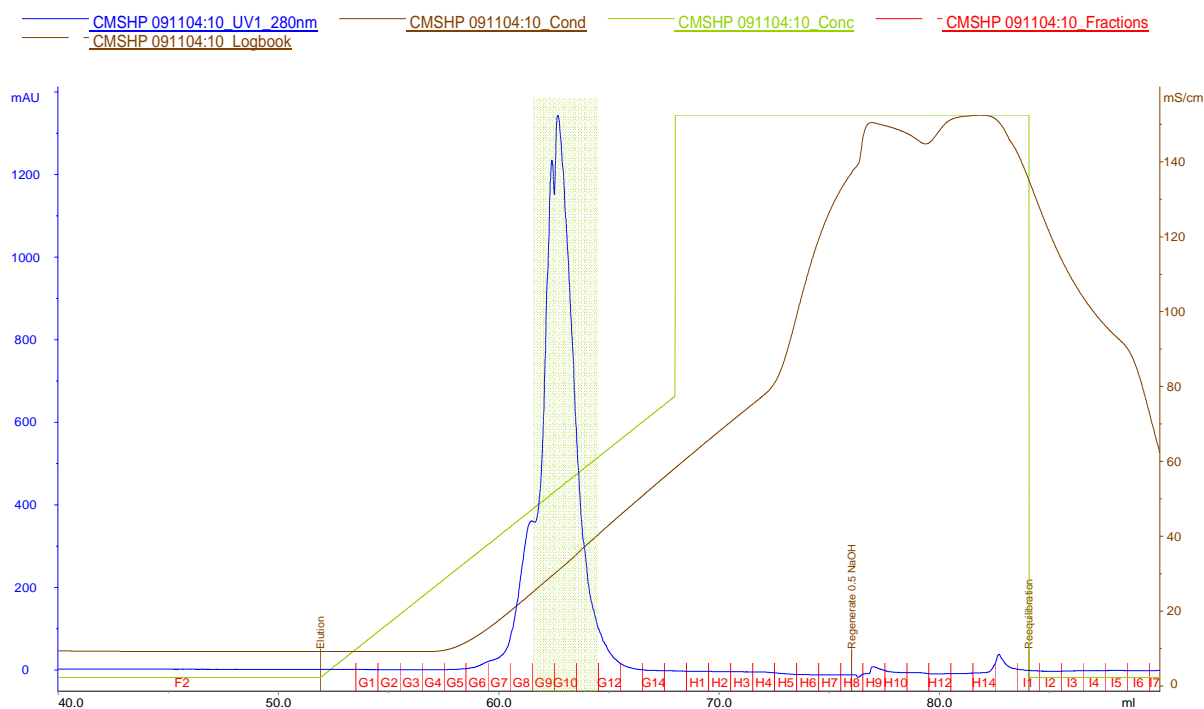
### 6.3.3.8 CIEX - CM Sepharose HP

CM Sepharose HP was tested because it is providing a weaker binding than the previous tested CIEX resins. A 1.6 mL (47 x 6.6 mm) column was used for testing. Blue Sepharose 6FF load was desalted using Amicon Ultra 10k desalting tubes to a conductivity of about 10 mS/cm and adjusted to pH of 5.5. The elution gradient was accomplished from zero to 50 % elution buffer in 10 CV (elution up to 1 M NaCl) and then 100 % elution buffer for two CV (elution with 2 M NaCl). Detailed method characteristics are shown in Table 29 and chromatogram with LDS-PAGE in Figure 29 and Figure 30.

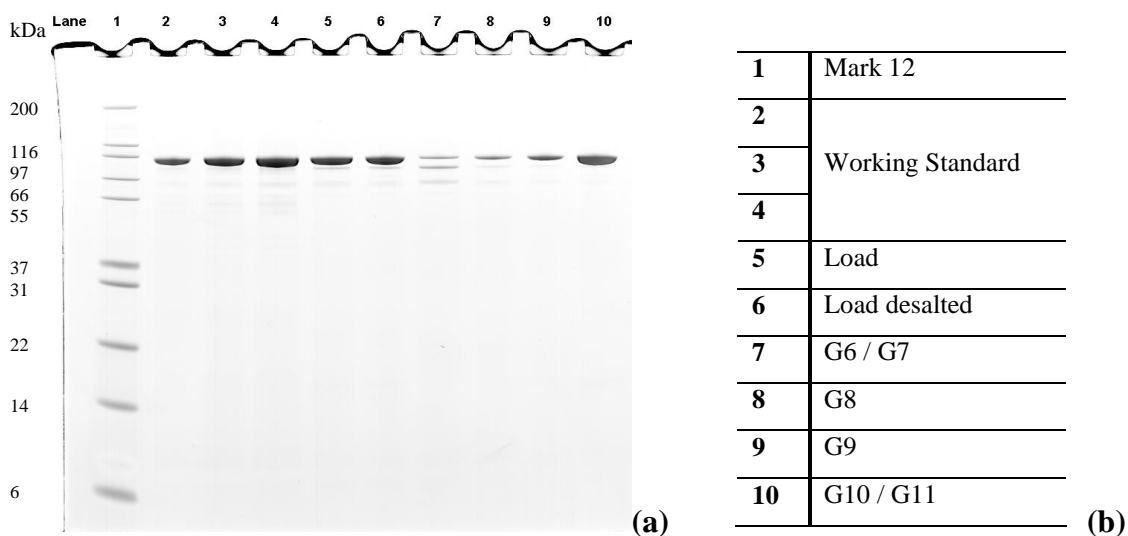
**Table 29: Method characteristics of CM Sepharose HP**

<b>Step</b>	<b>Buffer</b>	<b>Volume</b>	<b>Linear flow rate [cm/h]</b>
<b>Equilibration</b>	50 mM NaAc / 50 mM NaCl, pH 5.5	10 CV	200
<b>Load</b>	pH 5.5, $\sigma$ 10 mS/cm		100
<b>Wash</b>	50 mM NaAc / 50 mM NaCl, pH 5.5	10 CV	200
<b>Elution</b>	50 mM NaAc / 2 M NaCl, pH 5.5	12 CV	100
<b>Regeneration</b>	0.5 M NaOH	3 CV	100





**Figure 29: Chromatogram of CM Sepharos HP run: Fractions pooled from G9-G11**



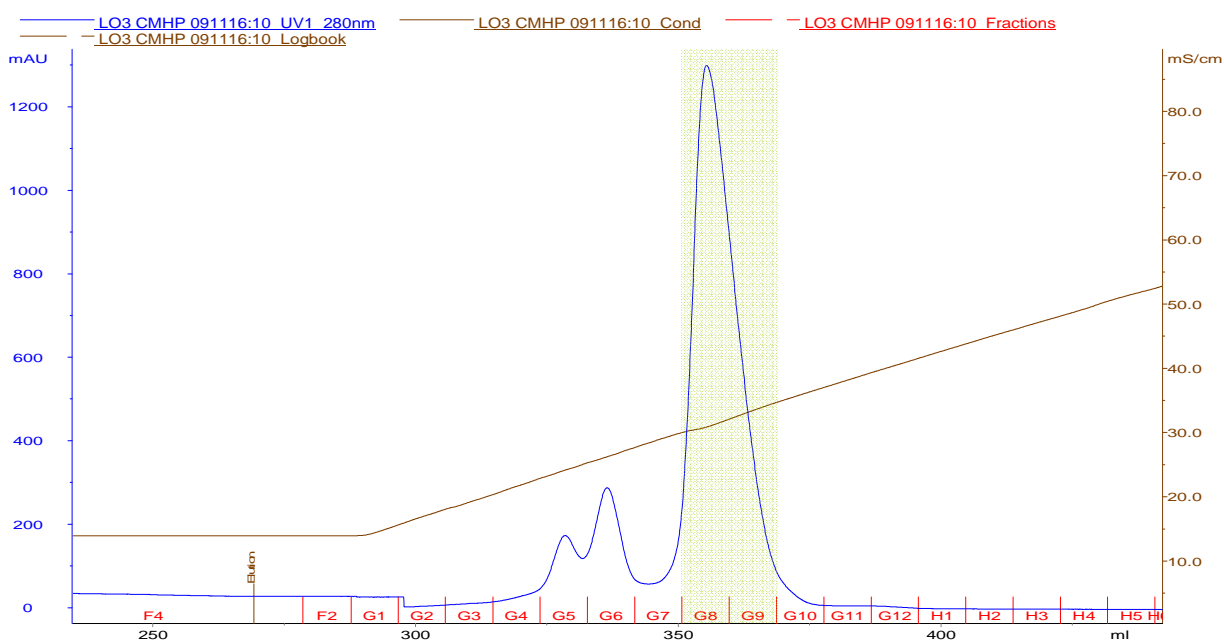
**Figure 30: Corresponding LDS-PAGE (a) with label (b)**

Elution of product already occurred at about 30 mS/cm, this is less than 0.5 M NaCl. The experiment showed that the protein could be completely eluted and sufficient depletion of impurity could be reached. The run resulted in a yield of 84.9 % and purity of 97.8 % analyzed by LDS-PAGE. On account of this good results the method of CM Sepharose HP was optimized concerning gradient slope.

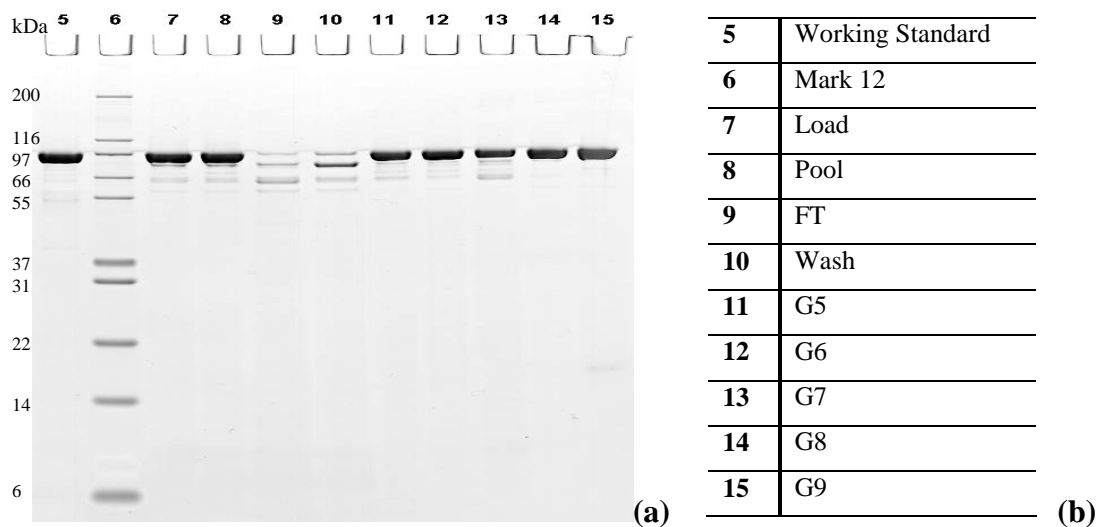
**Table 30: Optimized method characteristics of CM Sepharose HP**

Step	Buffer	Volume	Linear flow rate [cm/h]
<b>Equilibration</b>	50 mM NaAc / 100 mM NaCl, pH 5.5	10 CV	200
<b>Load</b>	pH 5.5, $\sigma$ 14 mS/cm		100
<b>Wash</b>	50 mM NaAc / 100 mM NaCl, pH 5.5	10 CV	200
<b>Elution</b>	50 mM NaAc / 1 M NaCl, pH 5.5	12 CV	100
<b>Regeneration 1</b>	2 M NaCl	3 CV	100
<b>Regeneration 2</b>	0.5 M NaOH	3 CV	100

The improved method is shown in Table 30 with corresponding chromatogram and LDS-PAGE in Figure 31 and Figure 32. Elution was programmed from 0 to 60 % elution buffer in 10 CV (elution up to 0.6 M NaCl) with a subsequent holding step at 60 % elution buffer for 2 CV. Thus decreasing the gradient slope from 8.5 to 5.1 mS/CV. The conductivity of the load was slightly increased to 14 mS/cm and the conductivity of the equilibration buffer was also increased, allowing impurities to be depleted in the washing step.



**Figure 31: Chromatogram of optimized CM Sepharose HP run: Fractions pooled from G8-G9**



**Figure 32: Corresponding LDS\_PAGE (a) with label (b)**

In all three elution peaks product was found. The remaining isoforms were separated with CM Sepharose HP, with the main peak containing the purified product. The experiments resulted up in yields between 84 % and 98 % and purities from 97-98 % measured by LDS-PAGE. As well Fractogel EMD TMAE was considered as intermediate step resin, but to obtain yields as high as with CM Sepharose HP, loading conductivity would have to be still reduced. Hence Fractogel EMD TMAE has no advantage over CM Sepharose HP. Due to this results, CM Sepharose HP was selected as intermediate step resin.

### 6.3.4 Present Downstream Process

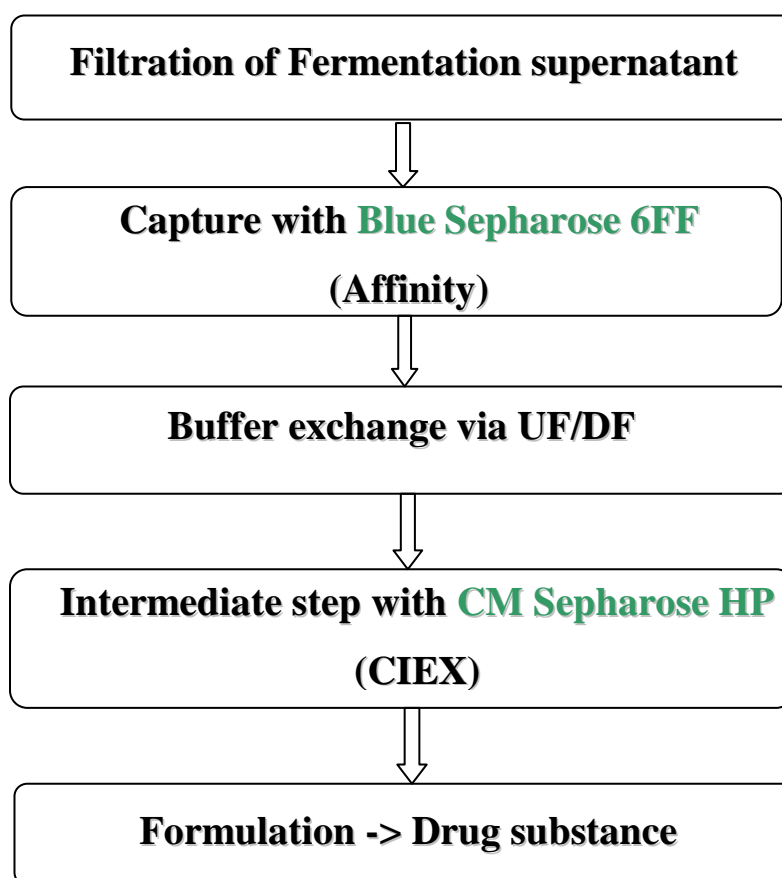
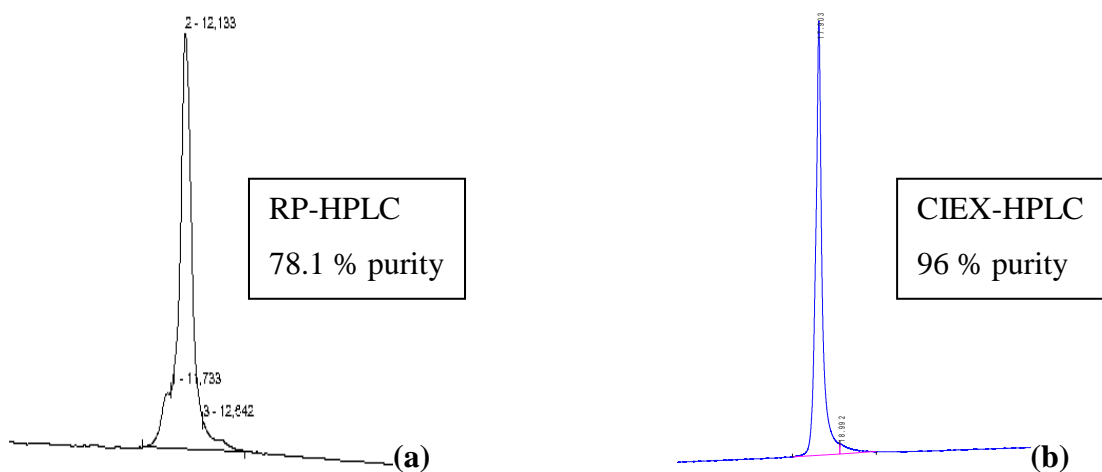


Figure 33: Flow chart of the current downstream process

Due to the obtained results the present downstream process, displayed in Figure 33, was chosen. After capture and intermediate step resins were specified, the complete purification process was tested. The aim was to produce 300-400 mg VHH3 material. Fermentation, capture and intermediate steps were processed as described above in the process development section. Desalting was made by ultra filtration / dia filtration (UF/DF) using a Labscale TFF system (Millipore, Billerica, USA) equipped with a Kwick Start 30 kDa UF membrane (GE Healthcare, Uppsala, Sweden). CM Sepharose HP equilibration buffer was used for the diafiltration step. Also the formulation step was carried out on a Labscale TFF system equipped with a 30 kDa membrane in 100 mM NaAc buffer, pH 5.5. Process results are shown in Table 31, calculated on the basis of LDS-PAGE analysis. An overall yield of 39 % or 314 mg could be achieved. In Figure 34 product purity profiles obtained by RP-HPLC and CIEX-HPLC are compared.

**Table 31: Outline over the complete downstream purification process**

Fraction	Volume [mL]	Concentration [mg/mL]	Product amount [mg]	Purification step	Step yield [%]	Purity [%]
<b>Fermentation supernatant = Load</b>	250	3,2	800	Fermentation	100	52
<b>Blue Sepharose 6FF Pool</b>	320	1,58	506	Capture	63	84
<b>UF/DF retentate = Load</b>	129	3,9	503	Desalting	100	77
<b>CM Sepharose HP Pool</b>	80	4,37	350	Intermediate	69	94
<b>Drug substance</b>	45	6,98	314	Formulation	90	98
					<b>Overall Yield</b>	<b>39 %</b>



**Figure 34: Purity of drug substance with RP-HPLC (a) and CIEX-HPLC (b)**

The results of the complete purification process are displayed in Table 31. An overall yield of 39 % with purities between 78.1-98 %, depending on the used analytical method, could be achieved. The present process obtained already good results, but still there is potential for optimization. It would be an advantage if the buffer exchange would be possible to eliminate in the process. Thus alternative media were tested, described in the following section.

## 6.4 Downstream Process - Alternatives

### 6.4.1 Intermediate Step – Mixed Mode Resins

Mixed-mode resins - Capto MMC, HEA HyperCel, PPA HyperCel and MEP HyperCel - were tested as alternative to the present media - CM Sepharose HP - for intermediate step. This mixed-mode resins are designed with multi-modal operating ligands with the possibility that adsorption takes place at high salt concentrations. Because the present downstream process requires a desalting step between capture and intermediate step, the replacement of CM Sepharose HP with a mixed-mode resin could make important savings in time and cost. On the other hand, the design of a well developed purification protocol is more complex by reason of the various interactions that take place simultaneous and that can change due to small changes in buffer composition.

#### 6.4.1.1 Capto MMC

Experiments were carried out using Blue Sepharose 6FF pool diluted with 50 mM NaAc to a conductivity between 75 - 80 mS/cm. Column volume was 8.2 mL (105 x 10 mm). In all experiments a product amount of 3.6 mg/mL gel was loaded. First experiments were made according to the suggested purification protocol (manuel of Capto MMC, GE Healthcare, NJ, USA; see Table 32) to localize the conditions for a reasonable DoE plan.

**Table 32: Screening conditions of Capto MMC**

<b>Equilibration</b>	Load and equilibration buffer 1 / 2 pH- units below pI of product
<b>Elution 1</b>	0.5 / 2 / 3 pH-units above pI of product
<b>Elution 2</b>	pH determined in Elution 1 + 0.5 / 1 / 1.5 M NaCl

The best results were maintained at high elution pH (9.5) and high salt concentration (1.5 M). The pH of equilibration buffer seemed to have little influence. As next step a DoE concept was created using a central composite design with full factorial approach within the range described in Table 33.

**Table 33: Condition boundaries for Capto MMC DoE concept**

	Minima	Maxima
<b>pH Equilibration buffer</b>	4.5	7
<b>pH Elution buffer</b>	7.5	10.5
<b>NaCl Elution buffer [M]</b>	0.7	2.1

Within the defined boundaries showed in Figure 35 the software created an experimental concept. All experiments were evaluated by LDS-PAGE. Only elution fractions with yield above 90 % (to be higher as the Blue Sepharose 6FF load) were pooled.

Std	Run	Type	Factor 1 A:pH equilibration buffer	Factor 2 B:pH elution buffer	Factor 3 C:NaCl elution buffer M
7	1	Fact	5.00	10.00	1.80
1	2	Fact	5.00	8.00	1.00
6	3	Fact	7.00	8.00	1.80
18	4	Center	6.00	9.00	1.40
2	5	Fact	7.00	8.00	1.00
4	6	Fact	7.00	10.00	1.00
15	7	Center	6.00	9.00	1.40
5	8	Fact	5.00	8.00	1.80
9	9	Axial	4.50	9.00	1.40
12	10	Axial	6.00	10.50	1.40
11	11	Axial	6.00	7.50	1.40
10	12	Axial	7.50	9.00	1.40
16	13	Center	6.00	9.00	1.40
13	14	Axial	6.00	9.00	0.70
8	15	Fact	7.00	10.00	1.80
17	16	Center	6.00	9.00	1.40
14	17	Axial	6.00	9.00	2.10
3	18	Fact	5.00	10.00	1.00

**Figure 35: DoE experimental plan for Capto MMC**

Results gained for yield and purity could be interpreted in different ways. Runs containing no fraction with product purity above the pooling criterion were not included in model calculation.. One way was to set all results that did not achieve the criterion of 90 % purity to zero (Figure 36 a) or to ignore all these results for calculation of the model (Figure 36 b).

Response 1 purity %	Response 2 yield %	Response 1 purity %	Response 2 yield %
100.00	72.94	100.00	72.94
0.00	0.00	0.00	0.00
91.30	2.66	91.30	2.66
0.00	0.00	0.00	0.00
0.00	0.00	0.00	0.00
96.20	6.61	96.20	6.61
0.00	0.00	0.00	0.00
0.00	0.00	0.00	0.00
0.00	0.00	0.00	0.00
97.00	105.84	97.00	105.84
0.00	0.00	0.00	0.00
91.14	8.32	91.14	8.32
91.81	7.43	91.81	7.43
0.00	0.00	0.00	0.00
98.57	66.25	98.57	66.25
90.53	8.01	90.53	8.01
97.95	20.65	97.95	20.65
98.67	30.96	98.67	30.96

**Figure 36: Results of completed DoE plan with different interpretations for analysis - use of all data (a); data that is not achieving pooling criterion is set to zero (b); data that is not achieving pooling criterion is excluded from analysis (c)**

Analysis of variance displays the significance of the approaches (see Table 34). All models are significant. The p-value describes how much influence a change of factor has to the model, lower p-values show higher influence.

**Table 34: Analysis of variance of Model a (a Yield; a Purity) and Model b (b Yield; b Purity)**

Source	R-Squared	p-value Prob > F	
<b>Model</b>	0.9485	0.0003	<b>significant</b>
<b>A-pH Equilibration buffer</b>		0.8550	
<b>B-pH Elution buffer</b>		< 0.0001	
<b>C-NaCl Elution buffer</b>		0.0030	

**(a Yield)**

Source	R-Squared	p-value Prob > F	
<b>Model</b>	0.6023	0.0040	<b>significant</b>
<b>A-pH Equilibration buffer</b>		0.0697	
<b>B-pH Elution buffer</b>		0.0028	
<b>C-NaCl Elution buffer</b>		0.0578	

**(a Purity)**



Source	R-Squared	p-value Prob > F	
Model	0.9213	0.0010	significant
A-pH Equilibration buffer		0.2129	
B-pH Elution buffer		0.0004	
C-NaCl Elution buffer		0.0067	

(b Yield)

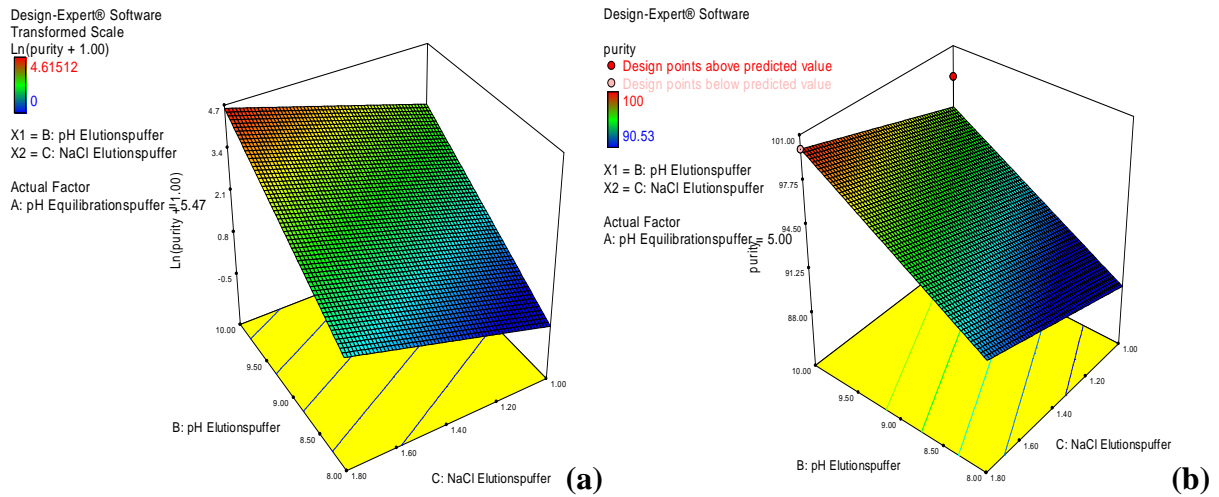
Source	R-Squared	p-value Prob > F	
Model	0.7799	0.0213	significant
A-pH Equilibration buffer		0.3271	
B-pH Elution buffer		0.0099	
C-NaCl Elution buffer		0.0719	

(b Purity)

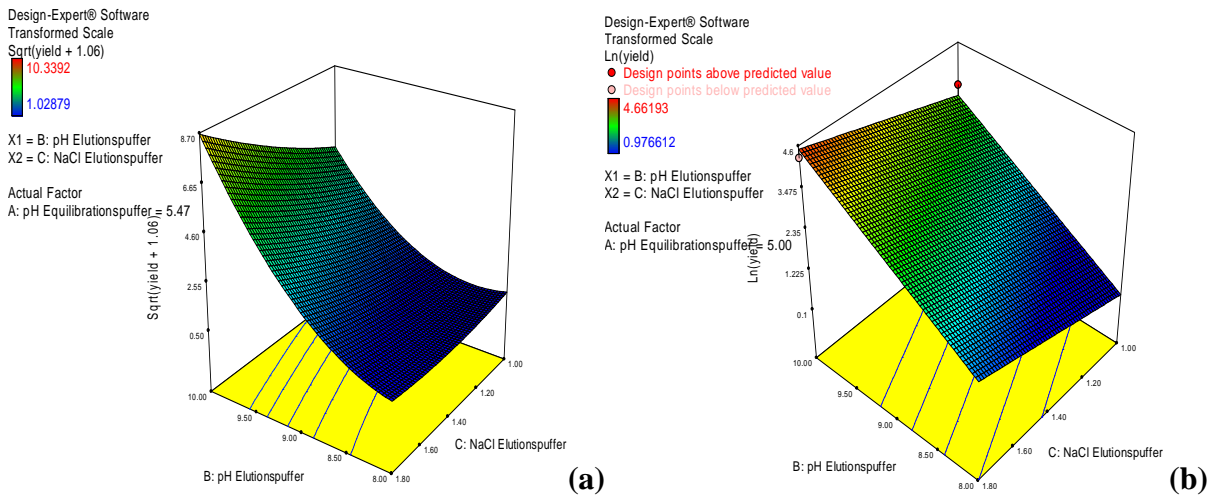
With these different evaluation approaches, the Design Expert 7 software was used to calculate the optimal buffer compositions to gain high results in yield and purity (Table 35). In Figure 37 and Figure 38 the 3D surface evaluation of the different approaches are displayed.

**Table 35: Comparison of the optimized results for the interpretation alternatives**

	Interpretation (a)	Interpretation (b)
pH Equilibration buffer	5.47	5
pH Elution buffer	10	10
NaCl Elution buffer [M]	1.8	1.8
Purity [%]	101.1	100.4
Yield [%]	75.8	91.0



**Figure 37: Purity overview of the different interpretation alternatives by 3D surface**



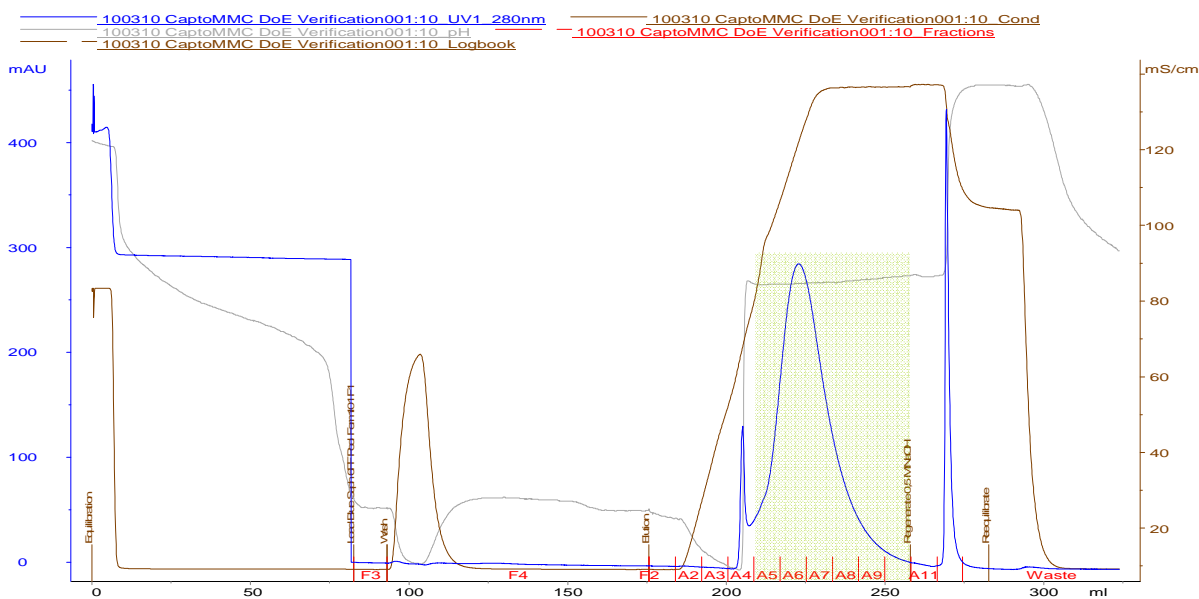
**Figure 38: Yield overview of the different interpretation alternatives by 3D surface**

Eight out of 18 runs did not achieve the pooling criterion. A too wide range was chosen to conduct the experiments. Both models give similar predictions with the chosen parameters. Yields of model b were higher, because the model was only calculated in the optimum range. Model b in comparison was calculated over the whole experimental space including all zero-results. A confirmation run with the calculated best buffer composition (interpretation b) was made, with method characteristics shown in Table 36 and chromatogram shown in Figure 39. The yield achieved was 104.7 % and the purity achieved was 99.4 % both measured by LDS-PAGE. Yield was much higher than predicted by the model, the purity was almost the same as predicted. Values over 100 % can be ascribed to analytical errors. As well the differences between predicted and reached values can happen due to the fact that LDS-PAGE is not an

exact analytical method with an error of around 20 %. To gain more accurate predictions a HPLC method should be applied in future with a new DoE plan within more narrow boundaries. Also the addition of additives to the elution buffer has to be considered, because the current best condition (pH 10, 1.8 M NaCl) is already harsh and could affect the protein stability.

**Table 36: Method characteristics of Capto MMC confirmation run**

Step	Buffer	Volume	Linear flow rate [cm/h]
<b>Equilibration</b>	50 mM NaAc / 50 mM NaCl, pH 5.0	10 CV	200
<b>Load</b>	pH 5.0, 75 mS/cm		150
<b>Wash</b>	50 mM NaAc / 50 mM NaCl, pH 5.0	10 CV	200
<b>Elution</b>	50 mM Glycin-NaOH / 1.8 M NaCl, pH 10.0	10 CV	200
<b>Regeneration</b>	0.5 M NaOH	3 CV	100



**Figure 39: Chromatogram of Capto MMC confirmation run: Pooled fractions from A5-A10**

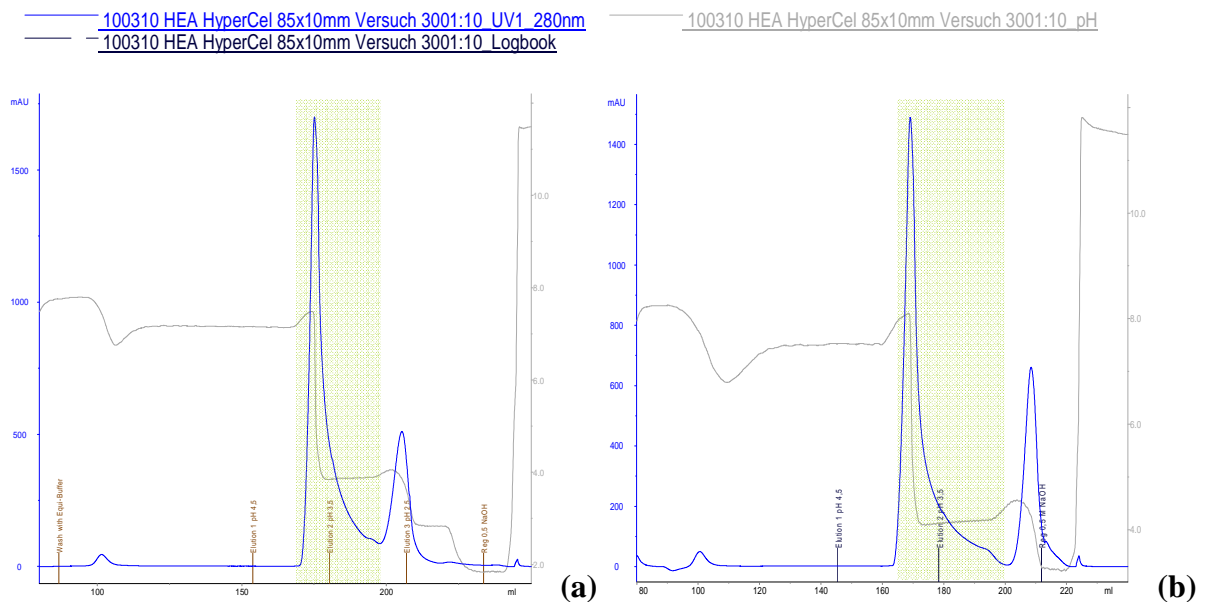
### 6.4.1.2 HEA HyperCel

Experiments were made with Blue Sepharose 6FF pool as load, once direct (conductivity 115 mS/cm) and once desalted by a Labscale TFF System (conductivity 25 mS/cm), always 10 mg product per mL gel were loaded. Method characteristics are displayed in Table 37.

**Table 37: Method characteristics of HEA HyperCel**

Step	Buffer	Volume	Linear flow rate [cm/h]
<b>Equilibration</b>	50 mM Tris-HCl, pH 8.0	10 CV	250
<b>Load</b>	pH 8.0, 25 / 115 mS/cm		150
<b>Wash</b>	50 mM Tris-HCl, pH 8.0	10 CV	250
<b>Elution 1</b>	50 mM NaAc / 50 mM NaCl, pH 4.5	4 / 5 CV	250
<b>Elution 2</b>	50 mM Glycin-NaOH / 50 mM NaCl, pH 3.5	4 / 5 CV	250
<b>Elution 3 *</b>	50 mM Glycin-NaOH / 50 mM NaCl, pH 2.5	4 CV	250
<b>Regeneration</b>	0.5 M NaOH	5 CV	80

\* was just performed with 25 mS/cm run

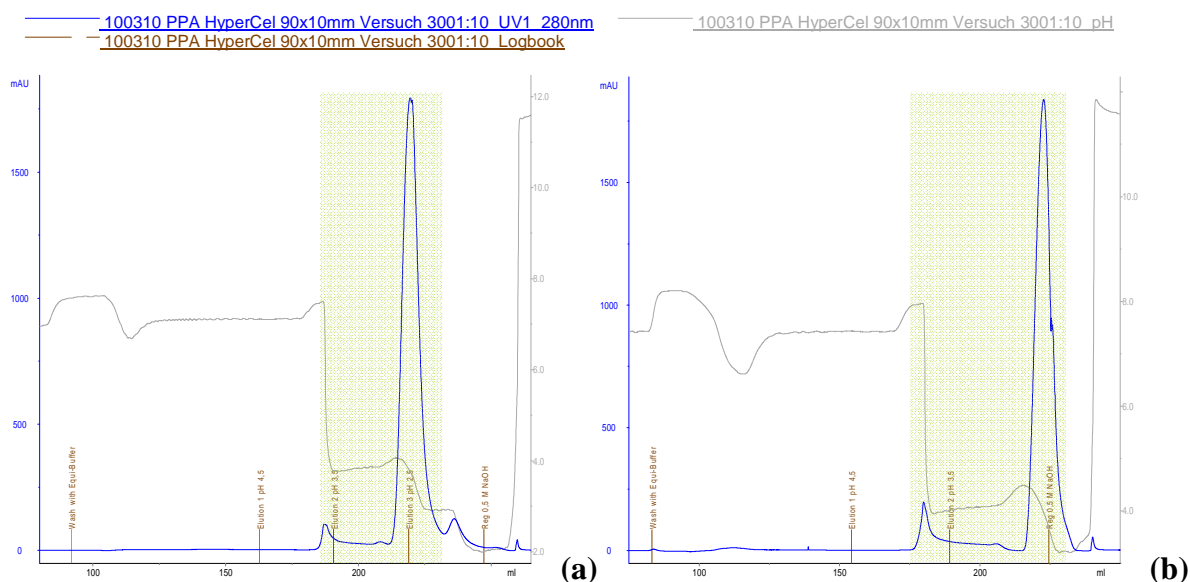


**Figure 40: Comparison HEA HyperCel – (a) 25 mS/cm; (b) 115 mS/cm**

Chromatograms (Figure 40) indicate that the direct load of Blue Sepharose 6FF pool makes no difference in product binding. Most of the product is eluted at pH 4.5 and some product along with by-products at pH 3.5. LDS-PAGE gave values of 78.5 % (25 mS/cm) and 74.0 % (115 mS/cm) for yield and 98.2 % purity for both conductivities. It appears that no desalting is needed for appropriate product binding and high yields.

### 6.4.1.3 PPA HyperCel

Experiments were conducted in the same way as experiments for HEA HyperCel with the same method characteristics (Table 37).

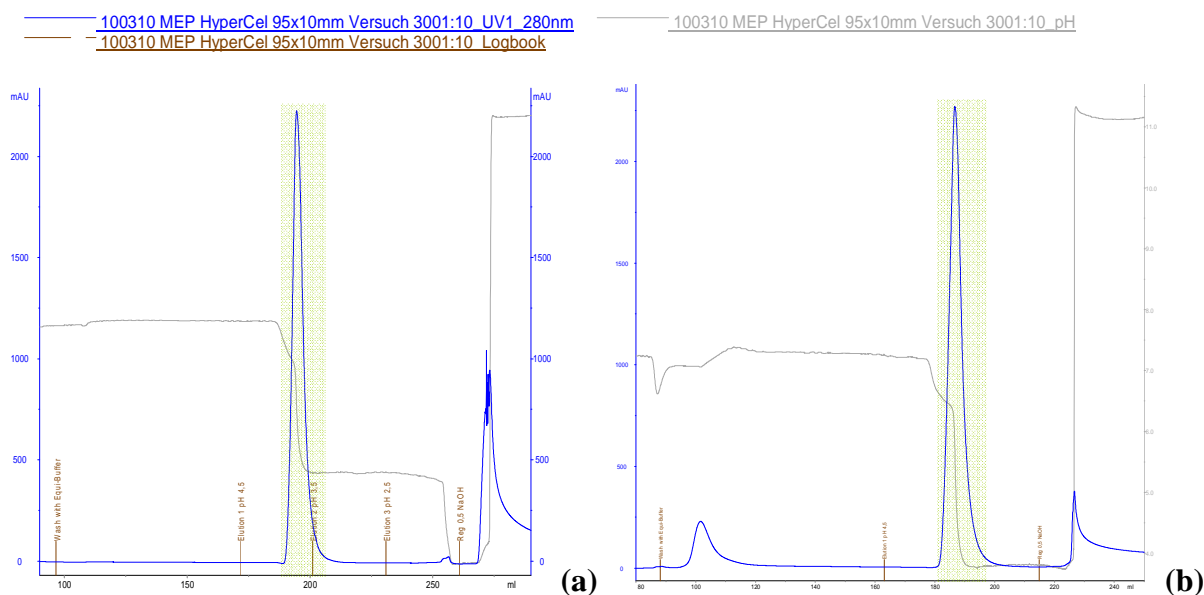


**Figure 41: Comparison PPA HyperCel – (a) 25 mS/cm; (b) 115 mS/cm**

Little of the product eluted at pH 4.5, most at pH 3.5 (Figure 41). By-products were separated at pH 2.5. The product eluted later from PPA HyperCel than from HEA HyperCel because the aromatic ligand of PPA HyperCel (phenylpropylamine) is more hydrophobic than the aliphatic ligand of HEA HyperCel (hexylamine). At a conductivity of 25 mS/cm a yield of 90.3 % and a purity of 97.5 % was achieved. At a conductivity of 115 mS/cm a yield of 87.4 % and a purity of 98.1 % was determined. The salt in the load seems to be required for binding and good results, higher conductivities had no negative effect.

### 6.4.1.4 MEP HyperCel

The experiments with MEP (4-Mercapto-Ethyl-Pyridine) HyperCel were conducted in the same way as experiments for HEA HyperCel and PPA HyperCel with the same method characteristics (Table 37), except that the run with high conductivity (115 mS/cm) in the load was only eluted at pH 4.5. Elution characteristics are shown in Figure 42.



**Figure 42: Comparison MEP HyperCel – (a) 25 mS/cm; (b) 115 mS/cm**

**Table 38: Results of MEP HyperCel runs**

Conductivity $\sigma$ [mS/cm]	Yield [%]	Purity [%]
25	74.7	97.9
115	95.1	98.9

The product eluted at pH 4.5. At high loading conductivity a small part of product was eluted in the wash fraction probably due to the conductivity change. At low loading conductivity the regeneration peak was much higher, possibly indicating stronger binding. LDS-PAGE displayed that yield and purity was higher with higher loading conductivity and lower with lower loading conductivity (Table 38). Again, like for the other tested mixed-mode resins, it is not necessary to desalt the load. For confirmation further investigation by repeating experiments would be needed.

## 6.4.2 Mixed Mode vs. CM Sepharose HP

Besides LDS-PAGE pools of the mixed-mode resins and CM Sepharose HP pool were compared by CIEX-HPLC (Figure 43), RP-HPLC (Figure 44) and LDS-PAGE silver staining (Figure 45). An overview of the results by the applied analytical methods gives Table 39.

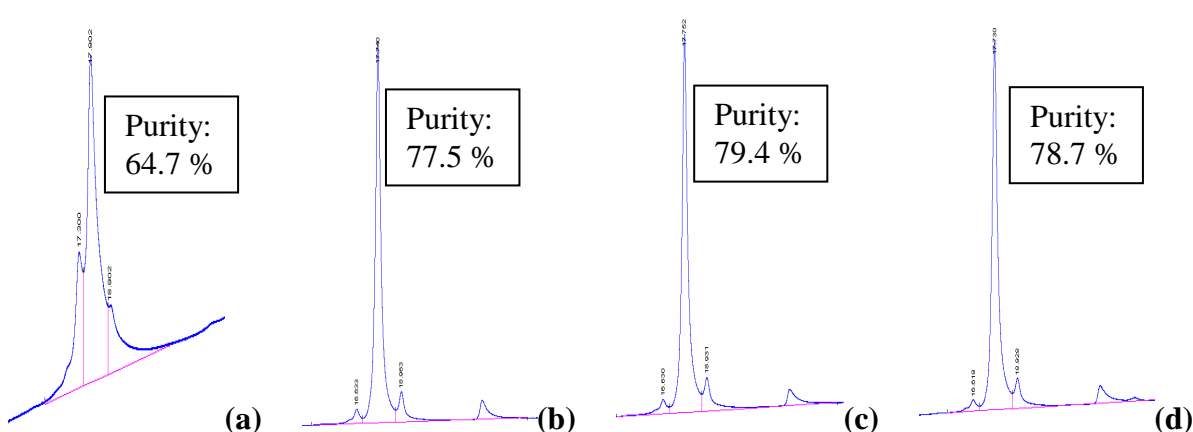


Figure 43: Purity overview of mixed-mode media for CIEX-HPLC - Capto MMC (a) HEA HyperCel (b) PPA HyperCel (c) MEP HyperCel (d)

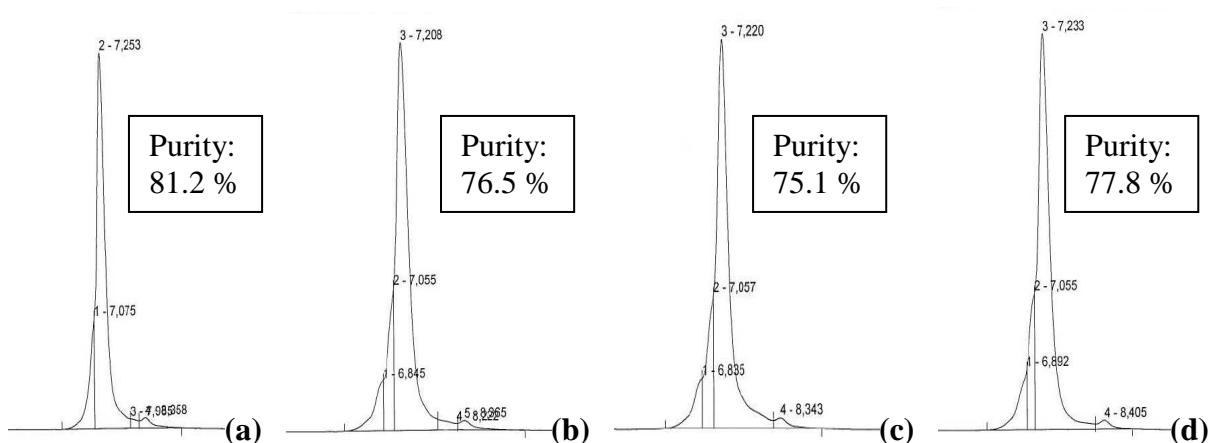
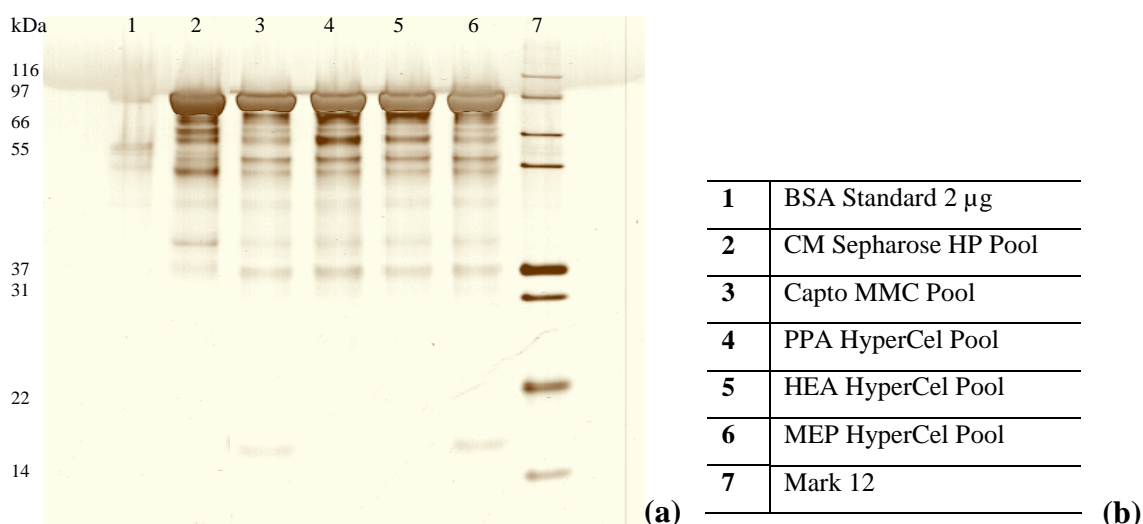


Figure 44: Purity overview of mixed-mode media for RP-HPLC - Capto MMC (a) HEA HyperCel (b) PPA HyperCel (c) MEP HyperCel (d)

The related RP-HPLC and CIEX-HPLC chromatograms of CM Sepharose HP (after formulation) are depicted in Figure 34 (page 62).

**Table 39: Comparison of mixed-mode media to CM Sepharose HP**

	LDS-PAGE Coomassie stained		CIEX-HPLC	RP-HPLC
	Ø Yield [%]	Ø Purity [%]	Purity [%]	Purity [%]
<b>Capto MMC</b>	104.7	99.4	64.7	81.2
<b>PPA HyperCel</b>	90.3	97.5	77.5	76.5
<b>HEA HyperCel</b>	76.3	98.2	79.4	75.1
<b>MEP HyperCel</b>	84.9	98.9	78.7	77.8
<b>CM Sepharose HP</b>	84.0	96.2	96.0	78.1

**Figure 45: Silver stained LDS-PAGE of mixed-mode media and CM Sepharose HP (a) with label (b)**

The results obtained for the mixed-mode resins were similar to CM Sepharose HP considering yield and purity. Values of purity analyzed by LDS-PAGE (Coomassie stained) were in the range of 97.5 to 99.4 % compared to 96.2 % of CM Sepharose HP. Analysis by RP-HPLC resulted in between 75.1 and 81.2 % compared to 78.1 % of CM Sepharose HP. Only purity analyzed by CIEX-HPLC still was lower of the mixed-mode resins (64.7-79.4 % compared to 96.0 %). Remaining isoforms were maybe only possible to analyze by CIEX-HPLC and not by RP-HPLC. This forms could be separated by CM Sepharose HP which is also a CIEX resin. Therefore the purity of the product after purification with CM Sepharose HP was higher as for the mixed-mode resins. The yields obtained by LDS-PAGE Coomassie stained varied between 76.3-104.7 % compared to 84.0 % for CM Sepharose HP. Silver staining (Figure 45; product amount per lane: 0.1 µg/µL) demonstrated similar band pattern,



Capto MMC and MEP HyperCel revealed one additional band at about 20 kDa in comparison to the band pattern of CM Sepharose HP. Stricter pooling criteria and the optimization of method characteristics are required before choosing one of the mixed-mode media as intermediate step. On all accounts there is the potential to replace CM Sepharose HP by one of the alternative sorbents and thereby eliminating the desalting step of the present purification process.

## ***7 Conclusions and Perspectives***

The design and development of a viable downstream process for the domain antibody  $V_{HH3}$  was successful. An overall yield of 39 % was achieved with purities between 78.1 % (RP-HPLC) and 98 % (LDS-PAGE). The high binding capacities confirmed the choice of HSA-affinity medium Blue Sepharose 6FF as the capture step resin. Kinetic values ( $q_{max}$ ,  $K_D$ ) of the tested capture resins MabSelect Xtra and Blue Sepharose 6FF were obtained from adsorption isotherms and accorded to data from literature. Intermediate step screening led to CM Sepharose HP as the intermediate step resin, but made a desalting step necessary in between the purification steps. Hence, an alternative to the utilized CIEX resin that could overcome the disadvantage of the present downstream process was needed. Novel chromatography resins, Capto MMC, PPA HyperCel, HEA HyperCel and MEP HyperCel were evaluated. These so-called mixed-mode medias possess multi-modal operating ligands allowing the possibility that adsorption takes place at high salt concentrations. All four chosen sorbents produced high yields (76.3 to 104.7) and purities (97.5 to 99.4 %) as analyzed by LDS-PAGE. As expected adsorption occurred at high salt concentrations (115 mS/cm). Silver staining as well demonstrated the similarity of  $V_{HH3}$  purification between all resins. Combining all obtained data suggested the possibility of replacing CM Sepharose HP by one of the novel mixed-mode resins. Further experiments and optimization are required to confirm these results and to be able to select one of the resins as a replacement to CM Sepharose HP. Furthermore, fluctuating analytical results and non-conformity require optimization of the applied analytical methods. Especially the analysis of the fermentation broth is posing a challenge to further experiments.

## 8 *Abbreviations*

ACN	Acetonitrile
AOX1	Aldehyde oxidase 1
BI RCV	Böhringer Ingelheim Regional Center Vienna
Bis-Tris	Bis(2-hydroxyethyl)-amino-tris(hydroxymethyl)-methane
C <sub>H</sub>	Constant fragment, heavy chain
C <sub>L</sub>	Constant fragment, light chain
CV	Column volume
DBC	Dynamic binding capacity
DCW	Dry cell weight
DoE	Design of experiments
EDTA	2,2',2'',2'''-(ethane-1,2-diyl)dinitrilo)tetraacetic acid
EtOH	Ethanol
F <sub>ab</sub>	Fragment antigen binding
F <sub>c</sub>	Fragment crystallizing / constant
FT	Flow through
GAP	Glyceraldehyde phosphate dehydrogenase promoter
HAc	Hydrogen acetate
HIC	Hydrophobic interaction chromatography
HPLC	High performance liquid chromatography
HQ-H <sub>2</sub> O	High quality water
HSA	Human serum albumin
Ig	Immunoglobulin
IPA	Isopropyl alcohol
kDa	Kilodalton
LDS-PAGE	Sodium dodecyl sulfate polyacrylamide gel electrophoresis
MCC	Metal chelate chromatography
MES	2-( <i>N</i> -morpholino)ethanesulfonic acid
NaAc	Sodium acetate
NaCl	Sodium chloride
NaOH	Sodium hydroxide

OD	Optical density
PBS	Phosphate buffered saline
PEG	Polyethylene glycol
pI	Isoelectric point
q	Capacity
RPC	Reversed phase chromatography
IEX	Ion exchange chromatography
RT	Room temperature
scF <sub>c</sub>	Single chain fragment crystallizing / constant
ACS	Acute coronary syndrome
SEC	Size exclusion chromatography
TFA	Trifluoroacetic acid
Tris	Tris(hydroxymethyl)aminomethane
V <sub>H</sub>	Variable fragment, heavy chain
V <sub>HH</sub>	Variable fragment, heavy chain only / camelid heavy-chain antibody
V <sub>L</sub>	Variable fragment, light chain
σ	Conductivity

## **9 Reference**

**Alberts, B., Johnson, A., Lewis, J., Raff, M., Roberts, K., Walter, P. (2002)** *Molecular Biology of the Cell* (4<sup>th</sup> edition). London: Garland Science.

**Arbabi Ghahroudi, M., Desmyter, A., Wyns, L., Hamers, R., Muyldermans, S. (1997)** Selection and identification of single domain antibody fragments from camel heavy-chain antibodies. *FEBS Lett* 414(3):521-526.

**Arbabi Ghahroudi, M., Desmyter, A., Wyns, L., Hamers, R., Muyldermans, S. (1997)** Selection and identification of single domain antibody fragments from camel heavy-chain antibodies. *FEBS Lett* 414(3):521-526.

**Bazl, M. R., Rasaee, M. J., Foruzandeh, M., Rahimpour, A., Kiani, J., Rahbarizadeh, F., Alirezapour, B., Mohammadi, M. (2007)** Production of chimeric recombinant single domain antibody-green fluorescent fusion protein in Chinese hamster ovary cells. *Hybridoma (Larchmt)* 26(1):1-9.

**Berg, J. M., Tymoczko, J. L., Stryer, L. (2002)** *Biochemistry* 5<sup>th</sup> ed. W. H. Freeman and Company, New York.

**Bird, P. A., Woodley, J. M., Sharp, D. C. A. (2002)** Monitoring and controlling biocatalytic processes, *BioPharm International* 15 (12), pp. 14-21.

**Cortez-Retamozo, V., Lauwereys, M., Hassanzadeh, G. G., Gobert, M., Conrath, K., Muyldermans, S., de Baetselier, P., Revets, H. (2002)** Efficient tumor targeting by single-domain antibody fragments of camels. *Int J Cancer* 98(3):456-462.

**Cos, O., Ramón, R., Montesinos, J., Valero, F. (2006)** Operational strategies, monitoring and control of heterologous protein production in the methylotrophic yeast *Pichia pastoris* under different promoters: a review. *Microb Cell Fact* 5:17.

**Cregg, J., Cereghino, J., Shi, J., Higgins, G. (2000)** Recombinant protein expression in *Pichia pastoris*. *Mol Biotechnol* 16:23-52.

**Cuatrecasas, P., Wilchek, M., Anfinsen, C. B. (1968)** Selective enzyme purification by affinity chromatography, *Proceedings of the National Academy of Sciences of the United States of America* 61 (2), pp. 636-643

**Cui, Y. and Walter, B. (2003)** Influence of albumin binding on the substrate transport mediated by human hepatocyte transporters OATP2 and OATP8, *J Gastroenterol*; 38:60–68.

**Dolk, E., van der Vaart, M., Lutje Hulsik, D., Vriend, G., de Haard, H., Spinelli, S., Cambillau, C., Frenken, L., Verrips, T. (2005)** Isolation of llama antibody fragments for prevention of dandruff by phage display in shampoo. *Appl Environ Microbiol* 71(1):442-450.

**Dumoulin, M., Conrath, K., van Meirhaeghe, A., Meersman, F., Heremans, K., Frenken, L. G., Muyldermans, S., Wyns, L., Matagne, A. (2002)** Single-domain antibody fragments with high conformational stability. *Protein Sci* 11(3):500-515.

**Ewert, S., Cambillau, C., Conrath, K., Pluckthun, A. (2002)** Biophysical properties of camelid VHH domains compared to those of human VH3 domains. *Biochemistry* 41(11):3628-3636.

**Fisher, R. A. (1966)** *The Design of Experiments*, 8th ed., Oliver & Boyd, London.

**Frenken, L. G., van der Linden, R. H., Hermans, P. W., Bos, J. W., Ruuls, R. C., de Geus, B., Verrips, C. T. (2000)** Isolation of antigen specific llama VHH antibody fragments and their high level secretion by *Saccharomyces cerevisiae*. *J Biotechnol* 78(1):11-21.

**Gagnon, P. in: Gottschalk, U. (Ed.) (2009)** Purification of Monoclonal Antibodies by Mixed-Mode Chromatography, in *Process Scale Purification of Antibodies*, John Wiley and Sons, New York, p. 125.

**Hahn, R., Bauerhansl, P., Shimahara, K., Wizniewski, C., Tscheliessnig, A., Jungbauer, A. (2005)** Comparison of protein A affinity sorbents II. Mass transfer properties, *Journal of Chromatography A*, 1093: 98-110.

**Hamers-Casterman, C., Atarhouch, T., Muyldermans, S., Robinson, G., Hamers, C., Songa, E. B., Bendahman, N., Hamers, R. (1993)** Naturally occurring antibodies devoid of light chains. *Nature*, 363: 446–448.

**Hamilton, S., Bobrowicz, P., Bobrowicz, B., Davidson, R., Li, H., Mitchell, T., Nett, J., Rausch, S., Stadheim, T., Wischnewski, H., Wildt, S., Gerngross, T. (2003)** Production of complex human glycoproteins in yeast. *Science* 301:1244-6.

**Harmsen, M. M. and De Haard, H. J. (2007)** Properties, production, and applications of camelid single-domain antibody fragments. *Applied Microbiology and Biotechnology*, 77: 13–22.

**Harmsen, M. M., van Solt, C. B., Fijten, H. P., van Keulen, L., Rosalia, R. A., Weerdmeester, K., Cornelissen, A. H., de Bruin, M. G., Eble, P. L., Dekker, A. (2007)** Passive immunization of guinea pigs with llama single-domain antibody fragments against foot-and-mouth disease. *Vet Microbiol* 120(3-4):193-206.

**Hohenblum, H., Borth, N., Mattanovich, D. (2003)** Assessing viability and cell-associated product of recombinant protein producing *Pichia pastoris* with flow cytometry. *J Biotechnol* 102:281-90.

**Holliger, P. and Hudson, P. J. (2005)** Engineered antibody fragments and the rise of single domains. *Nat. Biotechnol.*, 23, 1126-1136.

**Ismaili, A., Jalali-Javaran, M., Rasaee, M. J., Rahbarizadeh, F., Forouzandeh-Moghadam, M., Memari, H. R. (2007)** Production and characterization of anti-(mucin MUC1) single-domain antibody in tobacco (*Nicotiana tabacum* cultivar Xanthi). *Biotechnol Appl Biochem* 47(1):11-19.

**Janson, J. C. and Ryden, L. (1998)** Protein Purification: Principles, High-Resolution Methods, and Applications, Wiley-VCH Verlag GmbH, ISBN: 047118260 EAN: 9780471186267.

**Jobling, S. A., Jarman, C., The, M. M., Holmberg, N., Blake, C., Verhoeyen, M. E. (2003)** Immunomodulation of enzyme function in plants by single-domain antibody fragments. *Nat Biotechnol* 21(1):77-80.

**Joosten, V., Lokman, C., Van Den Hondel, C. A., Punt, P. J. (2003)** The production of antibody fragments and antibody fusion proteins by yeasts and filamentous fungi. *Microb. Cell Fact.*, 2, 1.

**Kleppmann W. (1998)** Taschenbuch Versuchsplanung, Produkte und Prozesse optimieren. Carl Hanser Verlag, München.

**Macauley-Patrick, S., Fazenda, M., McNeil, B., Harvey, L. (2005)** Heterologous protein production using the *Pichia pastoris* expression system. *Yeast* 22:249-70.

**Muyldermans, S. (2001)** Single domain camel antibodies: Current status. *J Biotechnol.* 74(4):277-302.

**Muyldermans, S., Baral, T. N., Cortez Retamozzo, V., De Baetselier, P., De Genst, E., Kinne J., Leonhardt, D., Magez, S., Nguyen, V. K., Revets, H., Rothbauer, U., Stijlemans, B., Tillib, S., Wernery, U., Wynsa, L., Hassanzadeh-Ghassabeh, G., Saerens, D. (2009)** Camelid immunoglobulins and nanobody technology, *Veterinary Immunology and Immunopathology* 128,178–183.

**Nguyen, V. K., Hamers, R., Wyns, L., Muyldermans, S. (2000)** Camel heavy-chain antibodies: Diverse germline VHH and specific mechanisms enlarge the antigen-binding repertoire. *Embo J* 19(5):921-930.

**Omidfar, K., Rasaei, M. J., Kashanian, S., Paknejad, M., Bathaie, Z. (2007)** Studies of thermostability in *Camelus bactrianus* (Bactrian camel) single-domain antibody specific for



the mutant epidermal-growth-factor receptor expressed by *Pichia*. *Biotechnol Appl Biochem* 46(1):41-49.

**Perez, J. M., Renisio, J. G., Prompers, J. J., van Platerink, C. J., Cambillau, C., Darbon, H., Frenken, L. G. (2001)** Thermal unfolding of a llama antibody fragment: A two-state reversible process. *Biochemistry* 40(1):74-83.

**Porath, J., Sundberg, L., Fornstedt, N., Olsson, I. (1973)** Salting-out in amphiphilic Gels as a new approach to hydrophobia adsorption, *Nature* 245 (5426), pp. 465-466.

**Rahbarizadeh, F., Rasaei, M. J., Forouzandeh, M., Allameh, A. A. (2006)** Overexpression of anti-MUC1 single-domain antibody fragments in the yeast *Pichia pastoris*. *Mol Immunol* 43(5):426-435.

**Revets, H., de Baetselier, P., Muyldermans, S. (2005)** Nanobodies as novel agents for cancer therapy. *Expert Opin Biol Ther* 5(1):111-124.

**Rios, M. (2007)** *Pharmaceut. Technol.* 40.

**Schmitz, U., Versmold, A., Kaufmann, P., Frank, H. G. (2000)** Phage display: a molecular tool for the generation of antibodies--a review. *Placenta*, 21 Suppl A, S106-S112.

**Scopes, R. K. (1994)** *Protein purification. Principles and practice*, 3rd, edn, Springer, New York.

**Soravia, S. and Orth A. (2006)** *Design of Experiments*. WILEY-VCH Verlag GMBH & Co. KGaA, Weinheim.

**Stanfield, R. L., Dooley, H., Flajnik, M. F., and Wilson, I. A. (2004)** Crystal Structure of a Shark Single-Domain Antibody V Region in Complex with Lysozyme. *Science*, 305: 1770-1773.

**Stijlemans, B., Conrath, K., Cortez-Retamozo, V., van Xong, H., Wyns, L., Senter, P., Revets, H., de Baetselier, P., Muyldermans, S., Magez, S. (2004)** Efficient targeting of conserved cryptic epitopes of infectious agents by single domain antibodies. African trypanosomes as paradigm. *J Biol Chem* 279(2):1256-1261.

**Taguchi, G. (1987)** System of Experimental Design, vols. I and II, Kraus International Publications, New York.

**Talamona A. (2005):** Laboratory Chromatography Guide. Büchi Labortechnik AG, Switzerland.

**Tschopp, J., Brust, P., Cregg, J., Stillman, C., Gingeras, T. (1987)** Expression of the lacZ gene from two methanol-regulated promoters in *Pichia pastoris*. *Nucleic Acids Res* 15:3859-76.

**van Bockstaele, F., Holz, J. B., Revets, H. (2009)** The development of nanobodies for therapeutic applications, *Current Opinion in Investigational Drugs* 10(11):1212-1224

**van der Linden, R. H., Frenken, L. G., de Geus, B., Harmsen, M. M., Ruuls, R. C., Stok, W., de Ron, L., Wilson, S., Davis, P., Verrips, C. T. (1999)** Comparison of physical chemical properties of llama VHH antibody fragments and mouse monoclonal antibodies. *Biochim Biophys Acta* 1431(1):37-46.

**Vu, K. B., Ghahroudi, M. A., Wyns, L., Muyldermans, S. (1997)** Comparison of llama VH sequences from conventional and heavy chain antibodies. *Mol Immunol* 34(16-17):1121-1131.

**Zhao, G., Xiao-Yan, D., Sun Y. (2009)** Ligands for mixed-mode protein chromatography: Principles, characteristics and design *Journal of Biotechnology* 144 3–11

## 10 Index of Figures

Figure 1: Composition of an IgG antibody [Joosten et al.] .....	- 10 -
Figure 2: Structure of an IgG antibody with its three active fragments [ <a href="http://www.secondary-antibody.com">http://www.secondary-antibody.com</a> ] .....	- 11 -
Figure 3: Variation of antibody fragments [P. Holliger et al., 2005] .....	- 12 -
Figure 4: Camelid heavy chain antibody and V <sub>HH</sub> domain antibody [S. Muyldermans et al., 2009] .....	- 13 -
Figure 5: Scheme of a 2 <sup>3</sup> fractional factorial design plus centre point (left) and a full central composite design (right) .....	- 20 -
Figure 6: Approximate molecular weight of the protein standard Mark 12 [ <a href="http://tools.invitrogen.com/content/sfs/manuals/mark12_card.pdf">http://tools.invitrogen.com/content/sfs/manuals/mark12_card.pdf</a> ] .....	- 22 -
Figure 7: Äkta explorer chromatography station [ <a href="http://www.gelifesciences.com/apatrix/upp01077.nsf/Content/aktadesign_platform~akta_explorer">www.gelifesciences.com/apatrix/upp01077.nsf/Content/aktadesign_platform~akta_explorer</a> ] .....	- 28 -
Figure 8: Growth and product formation of V <sub>HH3</sub> domain antibody.....	- 33 -
Figure 9: Representative chromatogram of MabSelect Xtra run: Fractions pooled from A12-B1 .....	- 35 -
Figure 10: Corresponding LDS-PAGE (a) of MabSelect Xtra run with label (b).....	- 35 -
Figure 11: Representative chromatogram of Blue Sepharose 6FF run: Fractions pooled from G8-G14 .....	- 37 -
Figure 12: Corresponding LDS-PAGE (a) of Blue Sepharose 6FF run with label (b) .....	- 37 -
Figure 13: Chromatogram of Blue Sepharose 6FF, competitive elution using sodium caprylate: Fractions pooled from L11-M12.....	- 38 -
Figure 14: Corresponding LDS-PAGE (a) of competitive Blue Sepharose 6FF run with label (b) .....	- 39 -
Figure 15: Breakthrough Curves at different velocities of Blue Sepharose 6FF: Curves were conducted using pre-purified product.....	- 41 -
Figure 16: Breakthrough Curves at different velocities of Mimetic Blue SA HL: Curves were conducted using pre-purified product.....	- 41 -
Figure 17: Breakthrough Curves at different velocities of MabSelect Xtra: Curves were conducted using pre-purified product.....	- 42 -

Figure 18: Dynamic binding capacity at 10 % breakthrough vs. residence time of Blue Sepharose 6FF, Mimetic Blue SA HL and MabSelect Xtra.....	- 42 -
Figure 19: Dynamic binding capacity at 10 % breakthrough vs. flow rate of Blue Sepharose 6FF, Mimetic Blue SA HL and MabSelect Xtra .....	- 43 -
Figure 20: Adsorption Isotherm of Blue Sepharose 6FF.....	- 45 -
Figure 21: Adsorption Isotherm of MabSelect Xtra.....	- 45 -
Figure 22: Chromatogram of Phenyl Sepharose HP run with 2 M NaCl equilibration: Fractions pooled from A5-A14 .....	- 48 -
Figure 23: Corresponding LDS-PAGE (a) with label (b).....	- 49 -
Figure 24: Comparison of Fractogel EMD TMAE runs – blue: 11 mS/cm; green: 26 mS/cm; pink: 38 mS/cm.....	- 50 -
Figure 25: Chromatogram of Q Sepharose FF run: Fractions pooled from A13-B5 .....	- 51 -
Figure 26: Comparison of Fractogel EMD SO <sub>3</sub> runs – blue: 9.2 mS/cm; green: 25 mS/cm; pink: 42 mS/cm.....	- 53 -
Figure 27: Corresponding LDS-PAGE Fractogel EMD SO <sub>3</sub> .....	- 53 -
Figure 28: LDS-PAGE of SP Sepharose HP (a) with label (b).....	- 55 -
Figure 29: Chromatogram of CM Sepharos HP run: Fractions pooled from G9-G11 .....	- 57 -
Figure 30: Corresponding LDS-PAGE (a) with label (b).....	- 57 -
Figure 31: Chromatogram of optimized CM Sepharose HP run: Fractions pooled from G8-G9 .....	- 58 -
Figure 32: Corresponding LDS_PAGE (a) with label (b).....	- 59 -
Figure 33: Flow chart of the current downstream process .....	- 60 -
Figure 34: Purity of drug substance with RP-HPLC (a) and CIEX-HPLC (b) .....	- 61 -
Figure 35: DoE experimental plan for Capto MMC.....	- 63 -
Figure 36: Results of completed DoE plan with different interpretations for analysis - use of all data (a); data that is not achieving pooling criterion is set to zero (b); data that is not achieving pooling criterion is excluded from analysis (c).....	- 64 -
Figure 37: Purity overview of the different interpretation alternatives by 3D surface.....	- 66 -
Figure 38: Yield overview of the different interpretation alternatives by 3D surface .....	- 66 -
Figure 39: Chromatogram of Capto MMC confirmation run: Pooled fractions from A5-A10..	- 67 -
Figure 40: Comparison HEA HyperCel – (a) 25 mS/cm; (b) 115 mS/cm .....	- 68 -
Figure 41: Comparison PPA HyperCel – (a) 25 mS/cm; (b) 115 mS/cm .....	- 69 -
Figure 42: Comparison MEP HyperCel – (a) 25 mS/cm; (b) 115 mS/cm .....	- 70 -

Figure 43: Purity overview of mixed-mode media for CIEX-HPLC - Capto MMC (a) HEA  
HyperCel (b) PPA HyperCel (c) MEP HyperCel (d) ..... - 71 -

Figure 44: Purity overview of mixed-mode media for RP-HPLC - Capto MMC (a) HEA  
HyperCel (b) PPA HyperCel (c) MEP HyperCel (d) ..... - 71 -

Figure 45: Silver stained LDS-PAGE of mixed-mode media and CM Sepharose HP (a) with  
label (b)..... - 72 -

## ***11 Index of Tables***

Table 1: Examples for half-life extension .....	- 14 -
Table 2: Overview of chromatography types .....	- 17 -
Table 3: Brief overview of mixed mode resins .....	- 18 -
Table 4: Components fixating solution .....	- 23 -
Table 5: YPG medium for <i>P. pastoris</i> .....	- 25 -
Table 6: OD Buffer .....	- 26 -
Table 7: Pipette scheme of adsorption isotherms .....	- 27 -
Table 8: Components of Äkta explorer .....	- 29 -
Table 9: Scening results .....	- 32 -
Table 10: Method characteristics of MabSelect Xtra capture step .....	- 34 -
Table 11: Results of MabSelect Xtra runs .....	- 35 -
Table 12: Method characteristics of Blue Sepharose 6FF capture step .....	- 36 -
Table 13: Results Blue Sepharose 6FF runs .....	- 37 -
Table 14: Method characteristics of competitive Blue Sepharose 6FF step .....	- 38 -
Table 15: Comparison of the dynamic binding capacity at 10 % breakthrough .....	- 43 -
Table 16: Comparison of capacities at 200 cm/h of tested affinity media .....	- 44 -
Table 17: Summarized engineering parameters of tested affinity media in comparison with data from literature .....	- 46 -
Table 18: Gel resins used for intermediate screening .....	- 47 -
Table 19: Method characteristics of Phenyl Sepharose HP .....	- 48 -
Table 20: Results Phenyl Sepharose HP runs .....	- 49 -
Table 21: Method characteristics of Fractogel EMD TMAE .....	- 50 -
Table 22: Results Fractogel EMD TMAE runs .....	- 51 -
Table 23: Result Q Sepharose FF runs .....	- 52 -
Table 24: Method characteristics of Fractogel EMD SO <sub>3</sub> .....	- 53 -
Table 25: Label of Fractogel EMD SO <sub>3</sub> LDS-PAGE .....	- 54 -
Table 26: Results Fractogel EMD SO <sub>3</sub> .....	- 54 -
Table 27: Method characteristics of SP Sepharose HP .....	- 55 -
Table 28: Results SP Sepharose HP runs .....	- 55 -
Table 29: Method characteristics of CM Sepharose HP .....	- 56 -
Table 30: Optimized method characteristics of CM Sepharose HP .....	- 58 -

Table 31: Outline over the complete downstream purification process .....	- 61 -
Table 32: Screening conditions of Capto MMC.....	- 62 -
Table 33: Condition boundaries for Capto MMC DoE concept.....	- 63 -
Table 34: Analysis of variance of Model a (a Yield; a Purity) and Model b (b Yield; b Purity) .....	- 64 -
Table 35: Comparison of the optimized results for the interpretation alternatives .....	- 65 -
Table 36: Method characteristics of Capto MMC confirmation run .....	- 67 -
Table 37: Method characteristics of HEA HyperCel.....	- 68 -
Table 38: Results of MEP HyperCel runs .....	- 70 -
Table 39: Comparison of mixed-mode media to CM Sepharose HP .....	- 72 -